NAVAL POSTGRADUATE SCHOOL
Monterey, California

THESIS

WELD POOL FLOW VISUALIZATION STUDIES
DURING GAS TUNGSTEN ARC WELDING
OF STEEL AND ALUMINUM

by

Peter E. Schupp

March, 1992

Thesis Advisor Y. Joshi

Approved for public release; distribution is unlimited.

T258653

REPORT DOCUMENTATION PAGE

Form Approved
OMB No. 0704-0188

1a REPORT SECURITY CLASSIFICATION: Unclassified

1b RESTRICTIVE MARKINGS:

2a SECURITY CLASSIFICATION AUTHORITY:

2b DECLASSIFICATION / DOWNGRADING SCHEDULE:

3 DISTRIBUTION / AVAILABILITY OF REPORT: Approved for public release; distribution is unlimited

4 PERFORMING ORGANIZATION REPORT NUMBER(S):

5 MONITORING ORGANIZATION REPORT NUMBER(S):

6a NAME OF PERFORMING ORGANIZATION: Naval Postgraduate School

6b OFFICE SYMBOL (If applicable): 34

7a NAME OF MONITORING ORGANIZATION: Naval Postgraduate School

6c ADDRESS (City, State, and ZIP Code): Monterey, Ca 93943-5000

7b ADDRESS (City, State, and ZIP Code): Monterey, Ca 93943-5000

8a NAME OF FUNDING / SPONSORING ORGANIZATION:

8b OFFICE SYMBOL (If applicable):

9 PROCUREMENT INSTRUMENT IDENTIFICATION NUMBER:

8c ADDRESS (City, State, and ZIP Code):

10 SOURCE OF FUNDING NUMBERS

PROGRAM ELEMENT NO	PROJECT NO	TASK NO	WORK UNIT ACCESSION NO

11 TITLE (Include Security Classification): WELD POOL FLOW VISUALIZATION STUDIES DURING GAS TUNGSTEN ARC WELDING OF STEEL AND ALUMINUM (Unclassified)

12 PERSONAL AUTHOR(S): Peter E. Schupp

13a TYPE OF REPORT	13b TIME COVERED	14 DATE OF REPORT (Year, Month, Day)	15 PAGE COUNT
Master's Thesis	FROM _____ TO _____	1992 March	69

16 SUPPLEMENTARY NOTATION: The views expressed in this thesis are those of the author and do not reflect the official policy or position of the DOD or the U.S. Government.

17 COSATI CODES		
FIELD	GROUP	SUB-GROUP

18 SUBJECT TERMS (Continue on reverse if necessary and identify by block number): Welding, Arc, Modeling, Flow Visualization, Fusion zone, Stirring

19 ABSTRACT (Continue on reverse if necessary and identify by block number)

A flow visualization study of current distribution effects on weld pool stirring in GTA steel welds is presented using a pulsed ultraviolet laser vision system. Weld pool stirring is almost eliminated in HY-80 steel by the use of symmetric current flow path within the weld samples. Periodic radial surface pulses are observed at low currents in stationary welds while flows of turbulent nature are observed at higher currents. Autogenous welds on 17.75 cm by 28.0 cm by 1.27 cm thick 6061 aluminum plates are also studied to determine resulting surface flow characteristics and weld pool growth rates. Clockwise stirring in conjunction with a vertical undulation is noted in stationary welds. Solidified weld zone exhibits a profound crater that was not present in welds on HY-80 Steel.

20 DISTRIBUTION / AVAILABILITY OF ABSTRACT: ☒ UNCLASSIFIED/UNLIMITED ☐ SAME AS RPT ☐ DTIC USERS

21 ABSTRACT SECURITY CLASSIFICATION: Unclassified

22a NAME OF RESPONSIBLE INDIVIDUAL: Y. Joshi

22b TELEPHONE (Include Area Code): (408) 646-3400

22c OFFICE SYMBOL: 69Ji

DD Form 1473, JUN 86 *Previous editions are obsolete.* S/N 0102-LF-014-6603

Approved for public release; distribution is unlimited.

Weldpool Flow Visualization Studies During Gas Tungsten Arc Welding of Steel and Aluminum

by

Peter E. Schupp
Lieutenant , United States Navy
B.S., California State Polytechnic University Pomona, 1982

Submitted in partial fulfillment
of the requirements for the degree of

MASTER OF SCIENCE IN MECHANICAL ENGINEERING

from the

NAVAL POSTGRADUATE SCHOOL
March 1992

ABSTRACT

A flow visualization study of current distribution effects on weld pool stirring in GTA steel welds is presented using a pulsed ultraviolet laser vision system. Weld pool stirring is almost eliminated in HY-80 steel by the use of symmetric current flow path within the weld samples. Periodic radial surface pulses are observed at low currents in stationary welds while flows of turbulent nature are observed at higher currents. Autogenous welds on 17.75 cm by 28.0 cm by 1.27 cm thick 6061 aluminum plates are also studied to determine resulting surface flow characteristics and weld pool growth rates. Clockwise stirring in conjunction with a vertical undulation is noted in stationary welds. Solidified weld zone exhibits a profound crater that was not present in welds on HY-80 steel.

TABLE OF CONTENTS

I. INTRODUCTION 1

II. EXPERIMENTAL APPARATUS AND PROCEDURE. 9

A. LASER VISION SYSTEM 9

1. LASER 9

2. IMAGE INTENSIFIER TUBE AND CAMERA 10

3. SYSTEM CONTROLLER 10

4. MONITOR AND RECORDER 12

B. WELDING SYSTEM 13

C. MATERIALS AND PROCEEDURE 14

1. HY-80 STEEL 14

2. 6061 ALUMINUM 15

III. STATIONARY ARC EXPERIMENTS 18

A. HY-80 STEEL 18

1. LOW CURRENT WELDS 18

2. MEDIUM CURRENT WELDS 20

3. HIGH CURRENT WELDS 24

B. 6061 ALUMINUM 26

1. LOW CURRENT WELDS 29

2. MEDIUM CURRENT WELDS. 29

3. HIGH CURRENT WELDS 30

C. WELDING EFFICIENCY 35

IV. MOVING ARC EXPERIMENTS 45
A. HY-80 STEEL 45
1. LOW CURRENT EXPERIMENTS 46
2. MEDIUM CURRENT EXPERIMENTS 47
3. HIGH CURRENT EXPERIMENTS 47
B. 6061 ALUMINUM 47
C. WELDING EFFICIENCY 50
V. CONCLUSIONS 53
LIST OF REFERENCES. 55
INITIAL DISTRIBUTION LIST.. 57

LIST OF TABLES

TABLE I. CHEMICAL COMPOSITION LIMITS FOR 6061 ALUMINUM. 16

TABLE II. SUMMARY LISTING OF LOW CURRENT STATIONARY ARC EXPERIMENTS ON HY-80 STEEL.. 21

TABLE III. PULSE FREQUENCY DATA FOR LOW CURRENT WELDS ON STEEL.. 23

TABLE IV. SUMMARY LISTING OF MEDIUM CURRENT STATIONARY ARC EXPERIMENTS ON HY-80 STEEL. 25

TABLE V. SUMMARY LISTING OF HIGH CURRENT STATIONARY ARC EXPERIMENTS ON HY-80 STEEL. 26

TABLE VI. SUMMARY LISTING OF LOW CURRENT STATIONARY ARC EXPERIMENTS ON 6061 ALUMINUM.. 31

TABLE VII. SUMMARY LISTING OF MEDIUM CURRENT STATIONARY ARC EXPERIMENTS ON 6061 ALUMINUM.. 34

TABLE VIII. SUMMARY LISTING OF HIGH CURRENT STATIONARY ARC EXPERIMENTS ON 6061 ALUMINUM.. 37

TABLE IX. SUMMARY LISTING OF CALCULATED EFFICIENCIES FOR STATIONARY ARC EXPERIMENTS ON 6061 ALUMINUM.. 44

TABLE X. SUMMARY LISTING OF MOVING ARC EXPERIMENTS ON HY-80 STEEL.. 46

TABLE XI. SUMMARY LISTING OF MOVING ARC EXPERIMENTS ON 6061 ALUMINUM.. 48

TABLE XII. SUMMARY LISTING OF CALCULATED EFFICIENCIES FOR MOVING ARC EXPERIMENTS ON 6061 ALUMINUM.. 52

LIST OF FIGURES

FIGURE 1. Asymmetric Current Path Geometry.. 6

FIGURE 2. Symmetric Current Path Geometry During GTAW 7

FIGURE 3. Progressively Asymmetrical Geometry. Positions of Electrodes (0-5) Show Increasing Non-Axisymmetric Effects in Current Flow Path. 8

FIGURE 4. Laser Photonics Pulsed nitrogen laser.. 11

FIGURE 5. Vacuum pump.. 11

FIGURE 6. Camera-Image Intensifier Tube.. 12

FIGURE 7. Controller, Monitor, and Recorder.. 13

FIGURE 8. Miller D.C. Welding Power Source. 14

FIGURE 9. Stationary arc grid arrangement for welds on aluminum.. 17

FIGURE 10. Moving arc layout for aluminum welds. Spacing between successive passes is identical.. 17

Figure 11. Time sequence of radial pulse phenomenon. 100A 11.2V 3mm Arc length 45 degree tip angle. Weld pool diameter 5.0 mm. Enlargement x18.0. 22

Figure 12. Sequence of circumferential oscillation. 235A 11.7V 3mm Arc length 45 degree tip angle. Weld pool diameter 13.1 mm. Enlargement x6.9.. 27

Figure 13. Etched Section Showing Inflection Of HY-80 Fusion Zone Interface. 198A, 11.3V, 15 mm Pool Diameter, 5.0mm Penetration Depth. Enlargement x6.6. 28

FIGURE 14. Weld Pool Growth Rate With Time For 6061 Aluminum Low Current Welds. 45 Degree Electrode Tip Angle, 3 mm Arc Length. 32

FIGURE 15. Weld Pool Growth Rate With Time For 6061. Expansion of 0-2 Second Interval From Figure 14. Aluminum Low Current Welds. 45 Degree Electrode Tip Angle, 3 mm Arc Length.. 33

Figure 16. Etched Section Showing Inflection Of 6061 Fusion Zone Interface. 150A, 11.2V, 5.53 mm Pool Diameter, 1.8mm Penetration Depth. Enlargement x7.55. 35

FIGURE 17. Weld Pool Growth Rate With Time For 6061 Aluminum Medium Current. 45 Degree Electrode Tip Angle, 3 mm Arc Length. 38

FIGURE 18. Weld Pool Growth Rate With Time For 6061. Expansion of 0-2 Second Interval From Figure 17 Aluminum Medium Current. 45 Degree Electrode Tip Angle, 3 mm Arc Length. . . . 39

FIGURE 19. Weld Pool Crossection Showing Large Conical Depression At High Current. 170A, 11.5V, Pool Diameter 12 mm, Penetration 6.5 mm. Enlargement x7.8 Times. 40

FIGURE 20. Weld Pool Growth Rate With Time For 6061 Aluminum High Current. 45 Degree Electrode Tip Angle, 3 mm Arc Length. 41

FIGURE 21. Weld Pool Growth Rate With Time For 6061. Expansion of 0-2 Second Interval From Figure 20. Aluminum High Current. 45 Degree Electrode Tip Angle, 3 mm Arc Length. . . . 42

FIGURE 22. Weld Pool Growth Rate With Time For 6061 Aluminum Low, Medium, and High Current. 45 Degree Electrode Tip Angle, 3 mm Arc Length. 43

FIGURE 23. Solidified Weld Bead on 6061 Aluminum Illustrating Weld Pool Rise, Depression, and Uneven Surface. 170A, 13.3V.. 49

Figure 24. Fusion Zone Of Moving Arc Weld On 6061 Aluminum. 150A, 11.2V, 2.0mm Penetration, 5.2 mm width, Welding Speed 1.78 mm/sec. Enlargement 6.3 times.. 50

I. INTRODUCTION

Many welding applications require extensive weld zone inspection to ensure reliable quality control. Present techniques such as x-ray photography, dye penetrant, ultrasonic, etc., are often time consuming and costly. Automatic adaptive control of the gas tungsten arc welding process would enable the welder to accurately detect and correct problems that cause sub standard quality welds on a real time basis eliminating the requirement for post-weld quality assurance testing. Ultimately this would lead to large savings in the money and effort that are required to produce certified welds.

The design of an automated weld inspection system requires a thorough understanding of the basic weld process. Fusion zone sizes, surface flow patterns, penetration depth, welding efficiency, etc are but a few of the parameters that must be known before an accurate theoretical representation can be developed. Many recent studies have attempted to mathematically model the gas tungsten arc welding process but have been limited by the fact that very little experimental data exists.

Oreper and Szekely presented a mathematical formulation for the fluid flow and temperature fields in a liquid pool during autogenous gas tungsten arc welding (GTAW) [Ref. 1].

Allowance was made for electromagnetic, bouyancy and surface tension forces in the weld. Numerical calculations predicted radially symmetric temperature and velocity fields within the cross-section of the weld pool.

Additional computations are reported by Saedi and Unkel [Ref. 2], Zacharia et al. [Ref. 3], and Kim [Ref. 4]. In all these studies the electromagnetic force field is considered to be axi-symmetric.

Relatively few experimental studies have been carried out to investigate the heat transfer and flow characteristics of weld pools. Woods and Milner conducted an extensive experimental study of the causes of motion in the weld pool beneath a tungsten arc [Ref. 5]. Lorentz forces were considered to be the primary cause of circumferential motion in the pool. The Lorentz force (F) is proportional to the vector cross product of the external magnetic field strength and the arc current strength.

$$F = jxB \qquad (2)$$

Where F = Lorentz force (N/m^3)
and j = current density (amp/m^2)
B = magnetic induction (Tesla)

A subsidiary cause of motion considered was the bouyancy force caused by temperature gradients within the molten material in the weld pool.

Malinowski et al. proposed that the alternating Lorentz force distribution causes an effect referred to as electromagnetic stirring within the liquid metal inside the weld pool [Ref. 6]. External magnetic fields were applied during GTA welding of austenitic stainless steel specimens by the use of Helmholtz coils in order to alter the Lorentz effect. A significant influence on the shape and size of resultant weld bead was noted. In addition, weld quality was found to be heavily dependent upon the strength and frequency of the induced magnetic field.

In a recent experimental study of GTAW by Espinosa [Ref. 7] rapid circumferential free surface rotation was observed in weld pools. The tests in this study were conducted using 2.54 cm thick HY-80 steel plate cut in to 28cm by 17.75cm sections. Stationary and moving arc experiments revealed a strong inter-relationship between current ground location and electromagnetic stirring of the weld pool free surface.

The Welding Handbook [Ref. 8] states that asymmetry in the weld piece current distribution path is the cause of a phenomenon called " arc blow ". In many situations the ground electrode is located in a position that causes a rapid change

of direction of the current flow path. This arrangement is responsible for a magnetic field near the weld pool which, it is hypothesised, induces rotational Lorentz forces. Figure 1 illustrates the direction of the current path during the welding of a flat work-piece. In this case, the lines of force are concentrated on the inside of the bend in the current path and are sparse on the outside of the curve. Hence, the magnetic field is much stronger on the side closest to the ground connection creating forces that could lead to rotation.

Asymmetric current paths appear to induce a stirring effect on the weld pool free surface and require modification of current computational models of the GTAW process. Experimentation to determine the relationship between current distribution and weld pool free surface flow patterns is essential to the refinement of present models. The creation of a symmetric magnetic field in the weld zone would allow the assessment of the relative effect that Lorentz forces have on stirring. One such symmetric arrangement is shown in Figure 2. In the situation depicted the direction of the current path remains unchanged throughout the weld zone. The resulting magnetic field is symmetric and should not induce rotational forces upon the pool provided the torch is stationary. In order to study the influence of progressively increased asymmetric current path upon stirring, the arrangement depicted in Figure 3 is introduced. Welds performed at the center of this circular plate would ensure axisymetric current

flow path within the pool, while welds away from the center would cause increasingly asymmetric current flow paths. In this situation minimal stirring should be observed in welds performed at the center while rotation should increase progressively as the welds are performed near the perimeter.

The primary objective of this study was to investigate the effect that asymmetric current paths have on electromagnetic stirring and surface flows in the weld pool. A symmetric current flow path was created in 2.54 cm thick by 30.5 cm diameter circular HY-80 steel plates and the resulting weld pool surface flow patterns were observed. Qualitative results were obtained for several welding power levels for stationary as well as moving arc welds.

Autogenous welds on 28 cm by 17.75 cm by 1.27 cm thick 6061 aluminum plate were also studied to determine surface flow patterns and weld pool growth rates. Information obtained from these experiments may serve as a source for the validation of future mathematical models of the GTA welding process on aluminum.

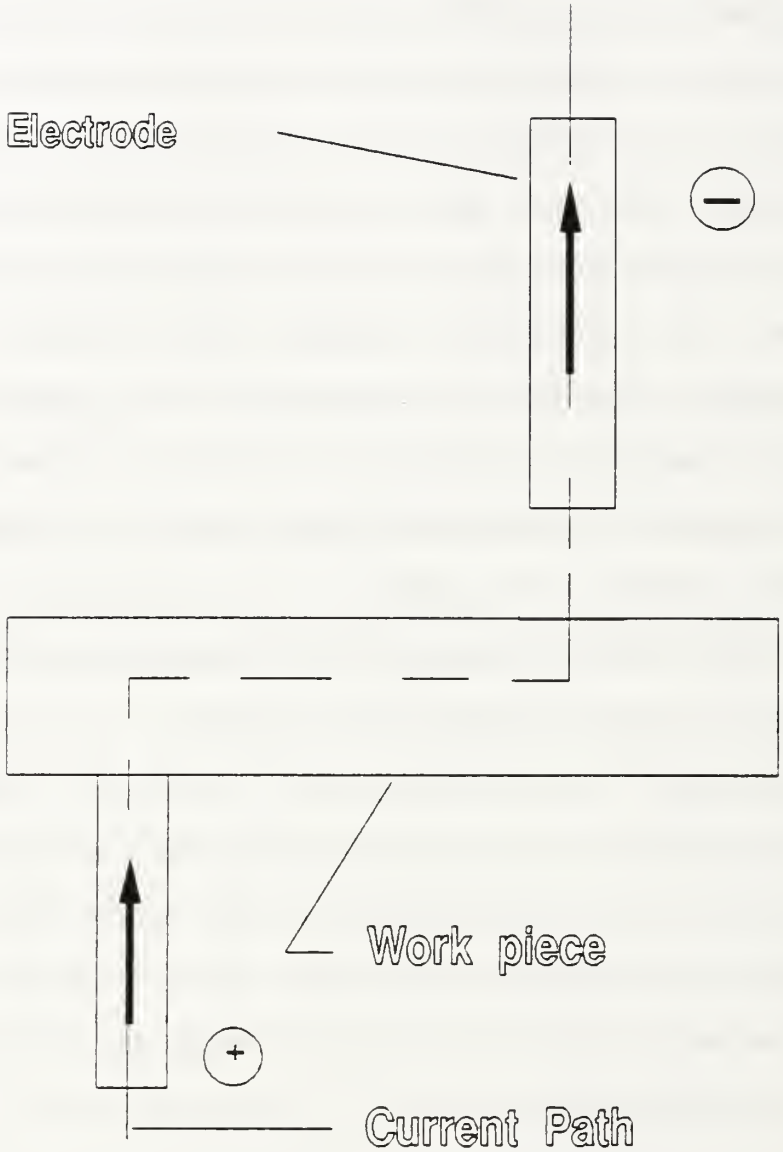

FIGURE 1: Asymmetric Current Path Geometry

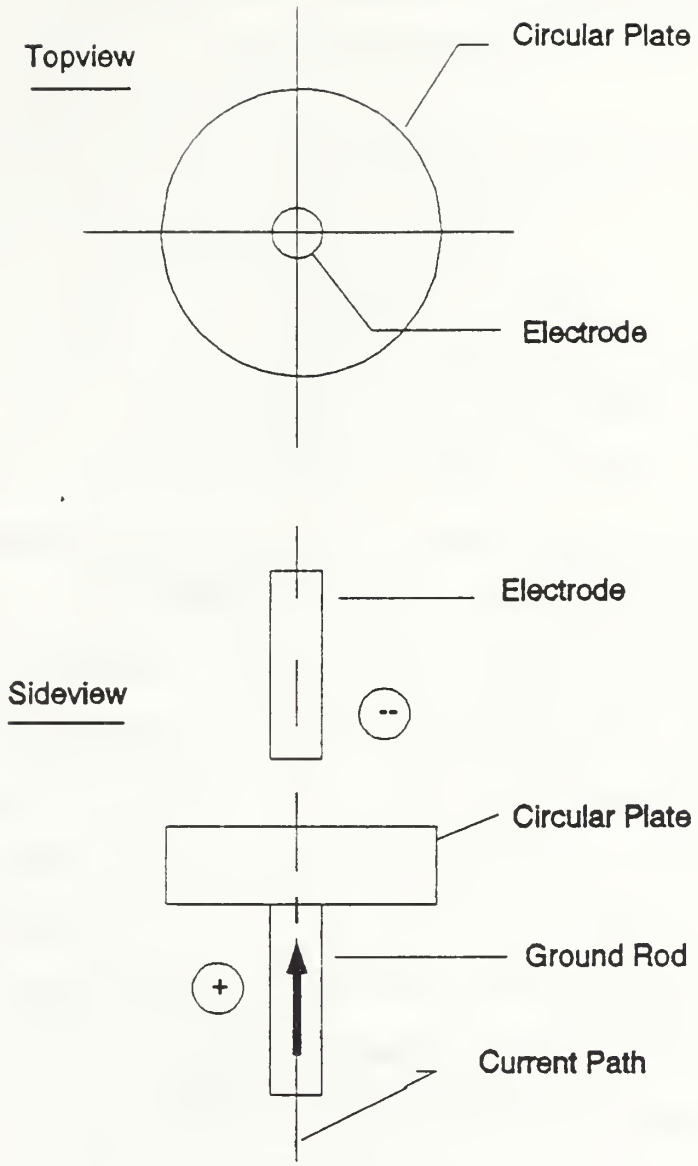

FIGURE 2: Symmetric Current Path Geometry During GTAW.

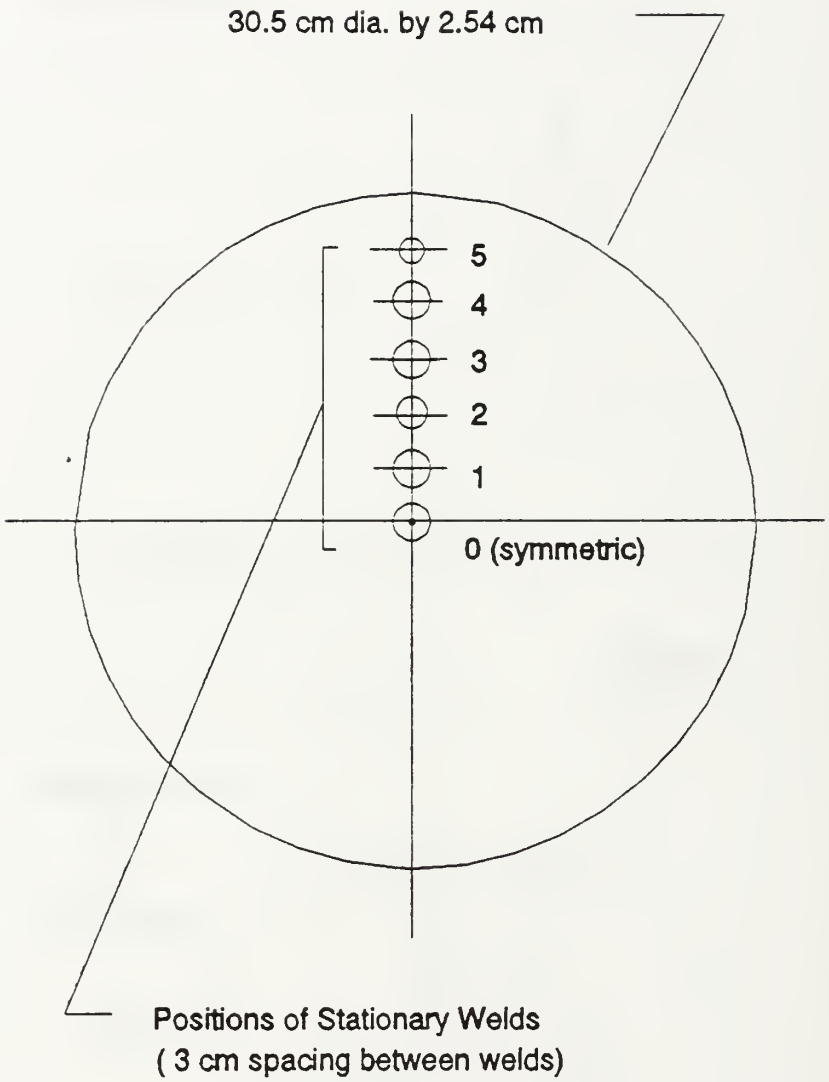

FIGURE 3. **Progressively Asymmetrical Geometry. Positions of Electrodes (0-5) Show Increasing Non-Axisymmetric Effects in Current Flow Path.**

II. EXPERIMENTAL APPARATUS AND PROCEDURE

A. LASER VISION SYSTEM

The vision system consisted of a Control Vision Inc. Model PN-232 Laser-Augmented Welding Vision system that included a pulsed nitrogen laser, an image intensifier tube, solid state video camera, video monitor, time lapse recorder, and a system controller. The theory of operation of the vision system is based on the concept that external illumination must be used to view an arc welding site because the light from the welding flash makes it impossible to obtain acceptable video imagery. Welding arc flash is overcome by the use of intense pulsed laser light in conjunction with appropriate shuttering and spectral filtering [Ref. 9].

1. LASER

A Laser Photonics PRA/Model UV12 Pulsed Nitrogen Laser was used as the light source for all experiments in this study. Optical laser radiation was produced in the near-ultraviolet region of the spectrum in 3 μs duration pulses at a rate of 60 Hz, a wavelength of 337.1 nm and an average power level of 90 mW. A continuous supply of nitrogen and a vacuum pump capable of maintaining 60 torr were also required [Ref. 10]. Figure 4 is a photograph of

the laser while Figure 5 is a photograph of the vacuum pump used.

2. IMAGE INTENSIFIER TUBE AND CAMERA

Electronic shuttering capability in addition to welding site image intensity amplification was provided by the image intensifier tube/camera. Image intensity was increased by as much as 10,000 to 1 with this equipment. The camera unit was a conventional CCD video sensor equipped with a narrow band optical filter that matched the laser light wavelength. This resulted in a combination of both temporal and spectral filtering [Ref. 9]. Figure 6 depicts the image tube and camera set up for a typical experiment.

3. SYSTEM CONTROLLER

The system controller transmitted the proper signals to fire the laser and control camera shuttering rate to ensure proper synchronization. An electronic time delay of 64 microseconds was used to compensate for inherent optical and electronic delays associated with the system. A shuttering rate of 60 frames per second enabled time lapse recording of weld pool motion.

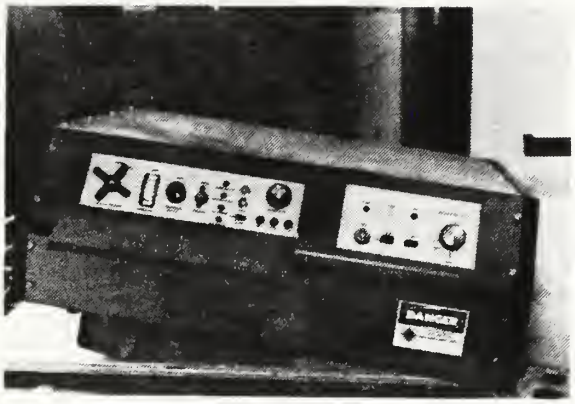

FIGURE 4. Laser Photonics Pulsed nitrogen laser.

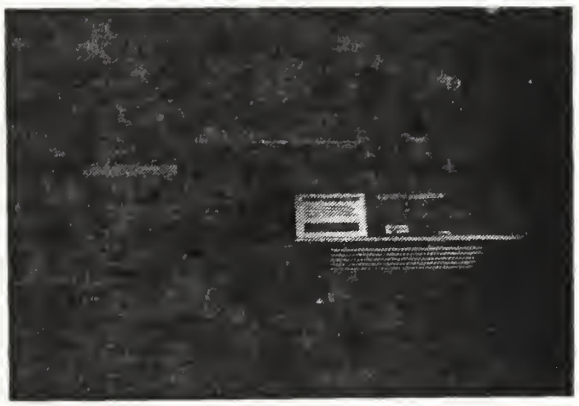

FIGURE 5. Vacuum pump.

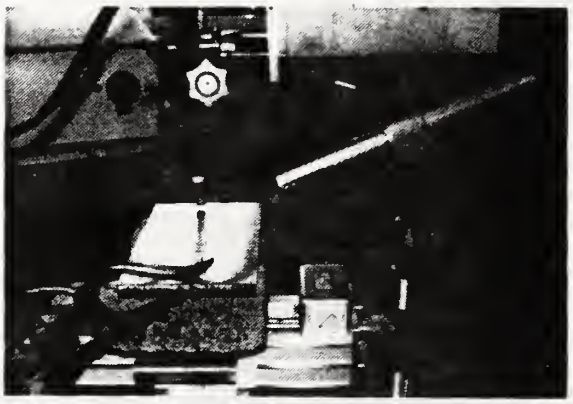

FIGURE 6. Camera-Image Intensifier Tube.

4. MONITOR AND RECORDER

The monitor used for viewing was a Panasonic Model TR-196M with a 19 inch screen. Recordings were made using a Panasonic Model AG-6720-P Time Lapse Recorder capable of frame by frame playback enabling weld pool growth rate data to be obtained directly from the monitor screen [Ref. 11]. Weld pool diameters were determined by measuring them directly from the monitor screen and converting them to actual sizes using a predetermined scale. Time sequence data was obtained by recording the number of frames between weld pool measurements. Surface flow sequences were acquired by taking black and white photographs of the video monitor. Figure 7 is a photograph of the system controller, monitor, and recorder.

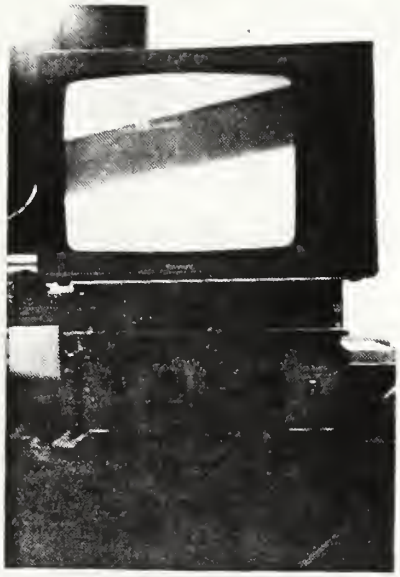

FIGURE 7. Controller, Monitor, and Recorder.

B. WELDING SYSTEM

A Miller Model SR600/SCMIA DC Welding Power Source with electroslope 3 and a Miller Digi-Meter Model 600 volt and 900 amp shown in Figure 8 was used for all welds. The Gas Tungsten Arc welding method was used because the weld pool surface is visible during the welding process. GTAW uses a nonconsumable tungsten electrode that is shielded with an inert gas. Argon was used as the shielding gas for all welds. The gas shield provides protection for the electrode and the molten weld pool and provides the required arc characteristics [Ref. 7].

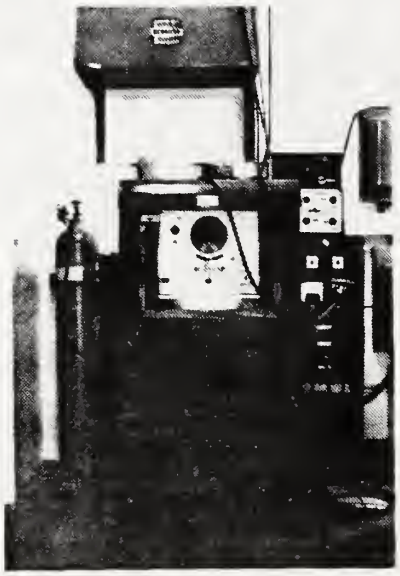

FIGURE 8. Miller D.C. Welding Power Source.

C. MATERIALS AND PROCEEDURE

1. HY-80 STEEL

HY-80 steel is described as a low carbon alloy steel with excellent strength and ductility that is ideal for use in the construction of naval vessels and other applications that involve dynamic loading [Ref. 12]. Results from a spectral chemical analysis of three representative samples of the HY-80 used in the present study were reported earlier [Ref. 8].

Stationary and moving arc welds were performed on 30.5 cm diameter by 2.54 cm thick circular plates. Symmetric

current path was created by locating a 3.80 cm diameter by 10.16 cm long solid cylindrical grounding shaft directly at the center of the plate. Static welds were performed at regular intervals of 3 cm along radial lines from the center of the plate. Moving arc welds were conducted by starting each weld 3 cm from the center of the plate and continuing outward toward the circumference on radial lines. Both stationary and moving arc experiments were conducted at low (100A nominal), medium (150A nominal), and high currents (200A nominal) in order to investigate the effects of input power on the surface flow patterns. Uncertainty in the measured current level was ± 5A, while uncertainty in the measured voltage was ± 0.2V.

2. 6061 ALUMINUM

6061 aluminum alloy is popular for seawater applications such as naval structures and exhibits excellent welding characteristics [Ref. 12]. Table I contains the acceptable chemical composition limits as quoted from the Department of Defense Structural Alloys Handbook.

Stationary and moving arc experiments were performed on 28 cm by 17.75 cm by 1.27 cm thick rectangular plates. Figure 9 indicates the grid arrangement that was used for stationary welds. In these tests welds were spaced 2.54 cm apart as shown in the photograph. Moving arc experiments were performed on rectangular plates of the same nominal

size but welds were conducted using the layout provided in Figure 10. Experiments with the aluminum were also performed at three different current levels (100A, 150A, and 170A) to study the input power effect on surface flow patterns. Uncertainty in the measured current level was ± 5A, while uncertainty in the measured voltage was ± 0.2V.

TABLE I: Chemical composition limits for 6061 aluminum.

ELEMENT	MINIMUM (% of total)	MAXIMUM (% of total)
Si	.40	.80
Mn	---	.15
Mg	.8	1.2
Ti	---	.15
Zn	---	.25
Cr	.04	.35
Fe	---	.7

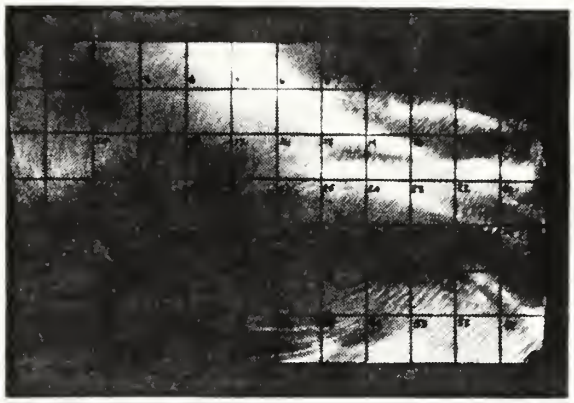

FIGURE 9. Stationary arc grid arrangement for welds on aluminum.

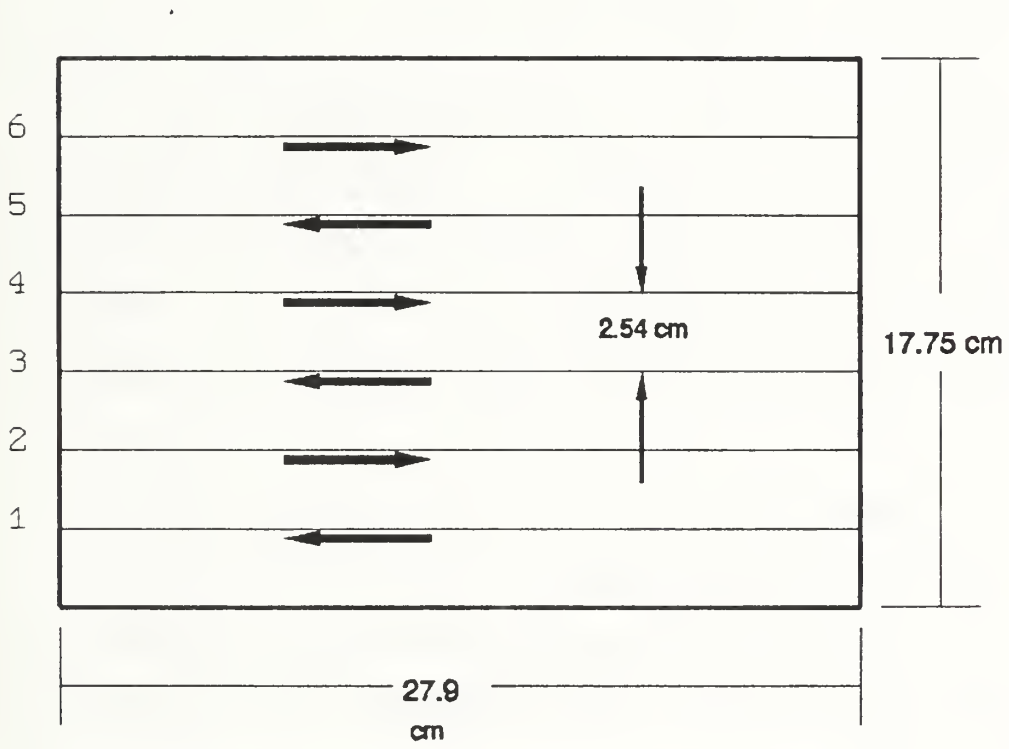

FIGURE 10. Moving arc layout for aluminum welds. Spacing between successive passes is identical.

III. STATIONARY ARC EXPERIMENTS

Stationary welds on 30.5 cm diameter by 2.54 cm thick circular HY-80 steel plates and 28 cm by 17.75 cm by 1.25 cm thick rectangular 6061 aluminum plates are considered in this chapter. Welds were conducted at low, medium, and high input current ranges for both materials. The effect of asymmetrical current path on surface flows was of primary interest in weld experiments on the steel while weld pool development, surface flow patterns, and welding efficiency values were studied in the tests conducted on aluminum. Weld pool size development with time was studied in detail for the aluminum welds. Flow visualization on the free surface was considerably more difficult on the aluminum due to the rapid build up of a heavy oxide layer on the surface.

A. HY-80 STEEL

1. LOW CURRENT WELDS

Welds were conducted for currents between 72 to 110 amps. Multiple spot welds of 3 to 5 minute duration each were performed at various locations starting at the center (totally symmetric current path) with successive welds placed away from the center along a radial line as described in Chapter II (increasingly asymmetric current path).

Shielding Gas (argon) flow rate was varied between .071 and .212 cubic meters per hour with no effect on surface flow patterns. Table II contains a summary of weld parameters and weld pool size results for this power range.

Surface flow visualization using the laser vision system for these currents (100A and 110A) revealed a smooth laminar weld pool with virtually no circumferential rotation in welds at or near the center of the plate. As the weld position was moved farther from the center of the plate sporadic rotation with unpredictable direction was observed in some instances.

A radial pulse phenomenon was observed in numerous welds at these power ranges (1.11kW and 1.12kW) and was independent of the location of the weld pool with respect to the center of the plate. Previously seeded particles of alumina periodically moved from the outside of the weld pool toward the center along annular rings. Figure 11 is a sequence of photographs taken at .0166 second intervals and illustrates the motion. White colored particles of alumina are seen forming on the surface near the circumference of the pool in the first photograph (a). The following pictures (b-f) show the alumina moving toward the center of the pool that is located directly below the V shaped electrode. The period was measured by counting the number of frames between pulses and ranged between .666 to 1.56 seconds for the

samples taken. A complete list of the period and frequency data of the sample pulses is contained in Table III.

Although a complete explanation for this motion does not exist, the inward radial direction suggests partial agreement with existing models. Zacharia et al. [Ref.13] indicate that fluid flow in the weld pool is due to a complex simultaneous interaction of the buoyancy, electromagnetic and surface tension gradients. Wang and Kou [Ref. 14] indicate that electromagnetic forces cause an inward radial motion while bouyancy forces result in an outward motion at the surface. Surface tension forces would normally produce an outward flow but the driving force can be reversed by surface active agents (chemical impurities such as sulfur) in the weld material. The inward pulsing motion observed in the present experiments may indicate an instability in the flows predicted by the models. Clearly, a transient computational model will be necessary to predict the observed flow patterns.

2. MEDIUM CURRENT WELDS

Medium current welds on HY-80 were conducted between 135 to 150 amps. The procedure was identical to that used for low current welds. Table IV contains a summary of weld parameters and size results for this power range.

TABLE II . SUMMARY LISTING OF LOW CURRENT STATIONARY ARC EXPERIMENTS ON HY-80 STEEL.

I (Amps)	V (Volts)	Power (Kwatts)	Arc Length (mm)	Weld Pool Diameter (mm)	Pool Depth (mm)	Argon Rate (cu.m/hr)
100	11.2	1.12	3	5.0	---	.071
100	11.2	1.12	3	5.9	---	.071
100	11.2	1.12	3	6.5	---	.071
100	11.2	1.12	3	6.5	---	.071
100	11.2	1.12	3	5.0	---	.071
100	11.2	1.12	3	6.0	---	.071
100	11.2	1.12	3	7.0	---	.071
100	11.2	1.12	3	5.9	---	.071
100	11.2	1.12	3	7.0	---	.142
100	11.2	1.12	3	6.5	---	.142
100	11.2	1.12	3	6.5	---	.142
100	11.2	1.12	3	7.0	---	.142
100	11.2	1.12	3	7.0	---	.142
110	11.1	1.11	3	7.0	---	.142
110	11.1	1.11	3	7.0	---	.142
110	11.1	1.11	3	5.5	---	.071
110	11.1	1.11	3	6.2	---	.071
110	11.1	1.11	3	7.5	---	.071
110	11.1	1.11	3	7.0	---	.071
110	11.1	1.11	3	7.0	---	.212
110	11.1	1.11	3	6.0	---	.212
110	11.1	1.11	3	7.0	---	.212
110	11.1	1.11	3	8.0	---	.212
110	11.1	1.11	3	8.0	---	.212
110	11.1	1.11	3	6.3	---	.212
110	11.1	1.11	3	7.5	---	.212

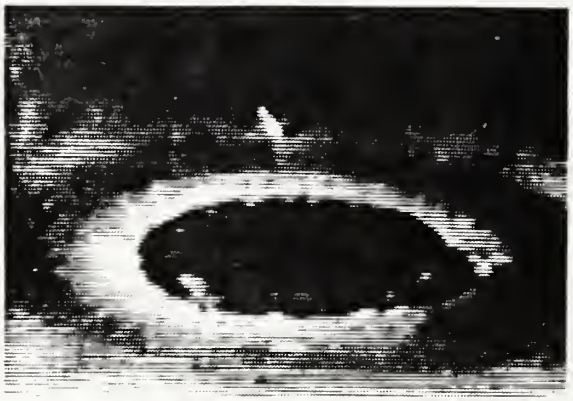

a. Time +0 seconds

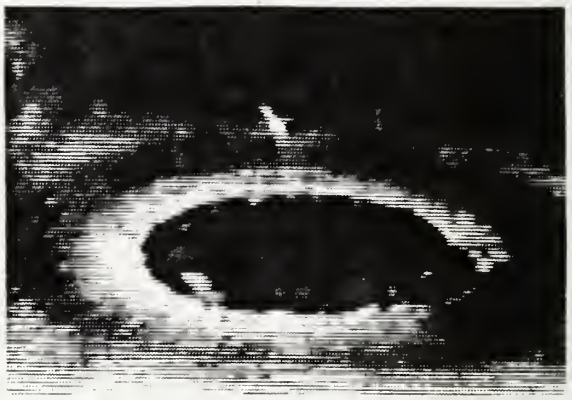

b. Time +.0166 seconds

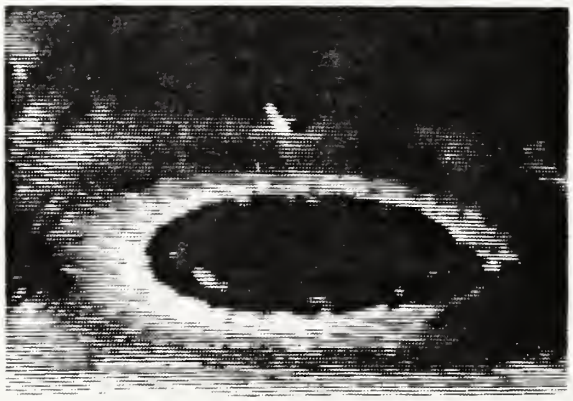

c. Time +.033 seconds

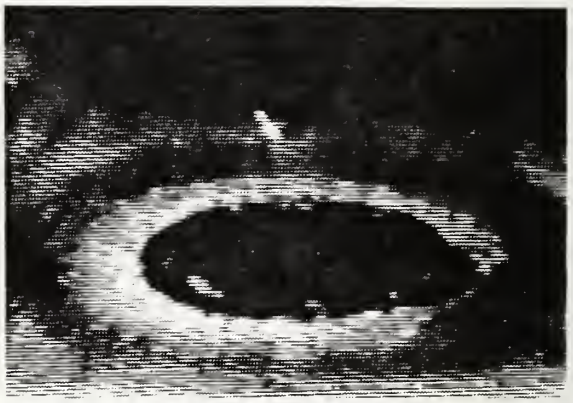

d. Time + .050 seconds

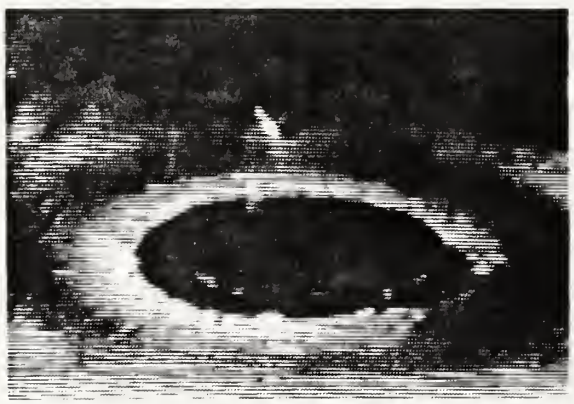

e. Time +.066 seconds

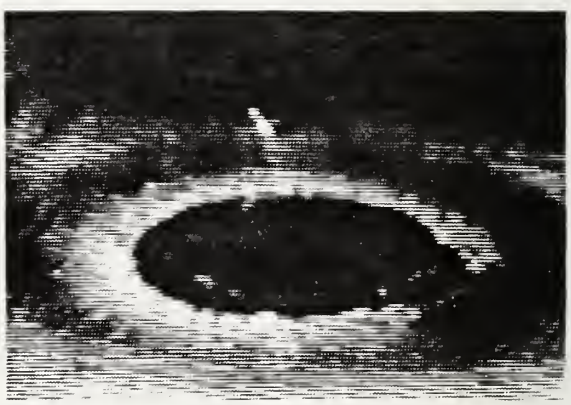

f. Time + .083 seconds

Figure 11. Time sequence of radial pulse phenomenon. 100A 11.2V 3mm Arc length 45 degree tip angle. Weld pool diameter 5.0 mm. Enlargement x18.0.

TABLE III. Pulse frequency data for low current welds on steel.

CURRENT (amps)	PERIOD (sec)	FREQUENCY (Hz)
100	1.0	1.0
100	1.0	1.0
100	0.85	1.176
100	1.2	0.833
100	1.37	0.735
100	1.56	0.641
100	0.93	1.072
100	1.0	1.0
100	0.98	1.02
110	1.0	1.0
110	0.86	1.155
110	0.80	1.25
110	0.81	1.235
110	0.85	1.176
110	0.67	1.50
110	0.91	1.10
110	1.55	0.645
110	1.5	0.667
110	1.53	0.667
110	1.0	1.0

Surface visualization revealed no rotation in weld pools at or near the center of the plate with minimal sporadic rotation occurring when the electrode was located near the

outer edge of the plate. Flows tended to be more active than at lower currents but particles of alumina on the surface were observed to remain in the same relative position for long periods of time (3 to 4 sec). In several instances particles were observed spinning about a local axis while rotation about the center of the pool was nonexistent.

3. HIGH CURRENT WELDS

High current welds were conducted between 198 to 235 amps. Table V contains a summary of parameters and results from welds in this power range.

Surface observations indicated considerably more vigorous flows than noticed in low and medium current welds. No pool stirring was observed in welds conducted near the center of the weld plate while weak intermittent rotation occurred when the electrode was near the outer edge. In many cases particles of alumina on the surface of the weld pool were observed remaining stationary within a small sector of the pool for relatively long periods. Figure 12 is a sequence of photographs taken at .0167 second intervals that shows a large white particle of alumina (located to the right of the electrode) maintaining the same relative position for .083 seconds (a-f). This clearly indicates a lack of rotation within the surface flows in the pool.

TABLE IV . SUMMARY LISTING OF MEDIUM CURRENT STATIONARY ARC EXPERIMENTS ON HY-80 STEEL.

I (Amps)	V (Volts)	Power (Kwatts)	Arc Length (mm)	Weld Pool Diameter (mm)	Pool Depth (mm)	Argon Rate (cu.m/hr)
150	12.0	1.8	3	9.5	---	.142
150	12.0	1.8	3	10.4	---	.142
150	12.0	1.8	3	11.0	---	.142
150	12.0	1.8	3	9.5	---	.142
150	12.0	1.8	3	10.0	---	.142
150	12.0	1.8	3	10.2	---	.142
150	12.0	1.8	3	9.0	---	.142
150	12.0	1.8	3	8.9	---	.142
150	12.0	1.8	3	9.0	---	.071
150	12.0	1.8	3	8.5	---	.071
150	12.0	1.8	3	9.5	---	.071
150	12.0	1.8	3	9.5	---	.071
150	12.0	1.8	3	10.0	---	.071
150	12.0	1.8	3	8.0	---	.071
150	12.0	1.8	3	9.5	---	.071
150	12.0	1.8	3	10.2	---	.071

Etched cross sections of several welds were obtained to study weld pool penetration and shape. Figure 13 shows an inflection point on the fusion zone interface that is symmetric about the pool vertical centerline. This is in keeping with a study by Zacharia et al. that predicts this shape as the result of a flow reversal within the weld pool due to the simultaneous interaction of buoyancy, surface tension, and electromagnetic forces [Ref. 13].

TABLE V . SUMMARY LISTING OF HIGH CURRENT STATIONARY ARC EXPERIMENTS ON HY-80 STEEL.

I (Amps)	V (Volts)	Power (Kwatts)	Arc Length (mm)	Weld Pool Diameter (mm)	Pool Depth (mm)	Argon Rate (cu.m/hr)
198	11.3	2.24	3	11.5	---	.142
198	11.3	2.24	3	12.0	---	.142
198	11.3	2.24	3	12.3	---	.142
198	11.3	2.24	3	12.0	---	.142
198	11.3	2.24	3	13.0	---	.142
198	11.3	2.24	3	13.0	---	.142
198	11.3	2.24	3	12.5	---	.142
198	11.3	2.24	3	14.1	4.0	.142
198	11.3	2.24	3	14.3	4.0	.142
205	13.0	2.67	3	14.5	---	.142
205	13.0	2.67	3	14.0	---	.142
205	13.0	2.67	3	14.5	---	.142
205	13.0	2.67	3	14.5	---	.142
205	13.0	2.67	3	15.0	---	.142
205	13.0	2.67	3	15.0	---	.142
205	13.0	2.67	3	15.0	---	.142
205	13.0	2.67	3	14.5	---	.142

B. 6061 ALUMINUM

As mention earlier, surface flows were more difficult to visualize than with the steel experiments, but several features unique to aluminum welds were detected:

* A slow vertical undulation of the pool surface was noted during the welding process.

* A crater shaped depression formed in the weld pool upon cessation of the welding arc and solidification of the material.

a. Time +0 seconds

b. Time +.0166 seconds

c. Time +.033 seconds

d. Time + .050 seconds

e. Time +.066 seconds

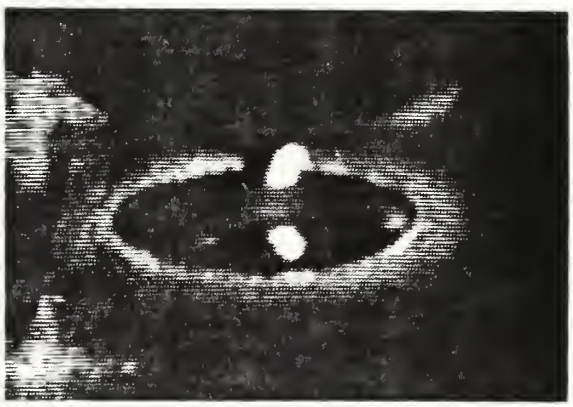

f. Time + .083 seconds

Figure 12. Sequence of circumferential oscillation. 235A 11.7V 3mm Arc length 45 degree tip angle. Weld pool diameter 13.1 mm. Enlargement x6.9

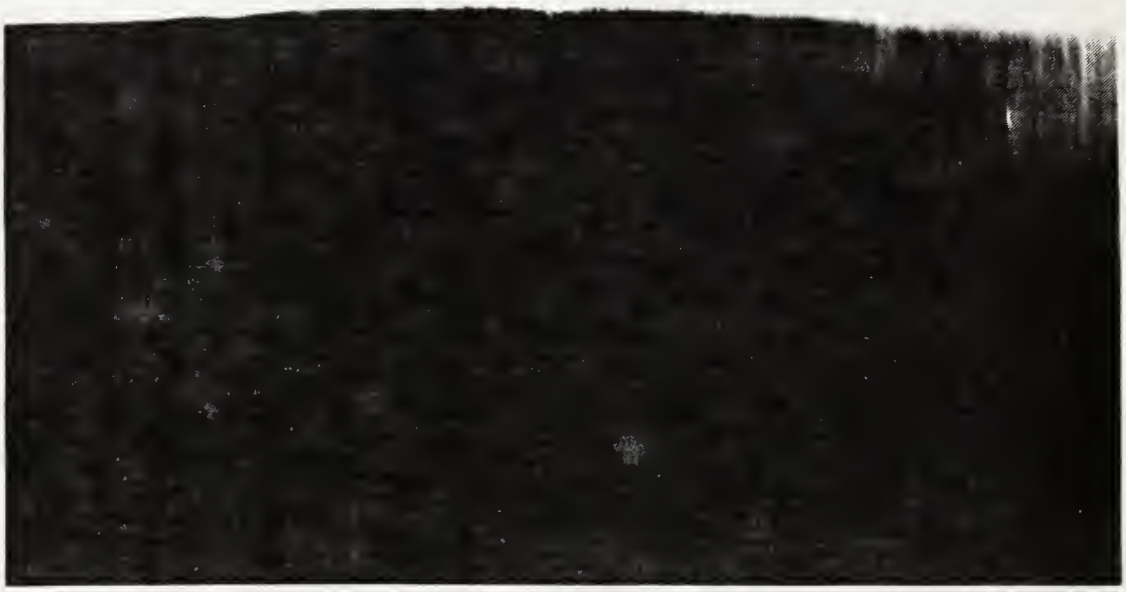

Figure 13. Etched Section Showing Inflection Of HY-80 Fusion Zone Interface. 198A, 11.3V, 15 mm Pool Diameter, 5.0mm Penetration Depth. Enlargement x6.6.

* Flow rotation in the weld pool was evidenced in several cases where molten material moved in the clockwise direction while underneath the surface oxide layer.

Weld pool growth rates were studied starting from the time an arc was struck until complete development of the pool had taken place. Comprehensive data in both tabular and graphical form is included in the following discussion for individual power ranges.

1. LOW CURRENT WELDS

Low current welds were conducted at 100 Amps, 11.5 and 16.4 Volts. Multiple spot welds of 30 to 60 seconds duration each were performed at various locations on rectangular plates as described in Chapter II. Shielding Gas (argon) flow rate was held constant at 0.425 cubic meters per hour for all experiments. Table VI contains a summary of weld parameters and fusion zone size results for this power range.

The weld pool was virtually impossible to distinguish from the surface oxide layer due to the very small size of the pool. Data obtained at this low current was limited to pool size development rates and has been presented graphically as Figures 14 and 15. Development was quite rapid at this power range with the pool reaching near steady state size of 5.9 millimeters in approximately 2.5 seconds. Small oscillations of 0.4 millimeters in magnitude about the fully developed pool are indicated in the curve at times greater than 3.0 seconds.

2. MEDIUM CURRENT WELDS.

Welds in this range were conducted at 150A, 11.2V. All other weld parameters and procedures were identical to low current aluminum welds. Table VII contains a summary of data for these experiments.

Vertical undulation of the weld and pool depression in the solidified material was noted at this power level. Figure 16 is an example of a typical weld pool section obtained and illustrates the weld pool depression. The pool and heat affected zone are clearly visible in this photograph with inflection points at the fusion zone interface present. Flow visualization revealed a distinct counter clockwise rotation of the molten material in several of the weld pools viewed. This motion was inferred by the observed movement of the surface oxide layer. Material beneath the oxide appeared to move around the pool in a circular pattern.

Weld pool development data was obtained and is presented graphically in Figures 17 and 18. A quasi-steady state diameter of 7.3 millimeters was reached between six to eight seconds after the arc was struck.

3. HIGH CURRENT WELDS

High current welds were conducted at 170 Amps, 11.5 volts. A summary of parameters and results is contained in Table VIII.

TABLE VI . SUMMARY LISTING OF LOW CURRENT STATIONARY ARC EXPERIMENTS ON 6061 ALUMINUM.

I (Amps)	V (Volts)	Power (Kwatts)	Arc Length (mm)	Weld Pool Diameter (mm)	Pool Depth (mm)
100	11.5	1.15	3	3.0	1.0
100	11.5	1.15	3	4.5	1.0
100	11.5	1.15	3	3.5	1.5
100	11.5	1.15	3	2.4	0.5
100	11.5	1.15	3	3.9	1.0
100	16.4	1.64	3	5.7	---
100	16.4	1.64	3	5.5	---
100	16.4	1.64	3	5.4	---
100	16.4	1.64	3	6.0	---
100	16.4	1.64	3	5.9	---
100	16.4	1.64	3	5.4	---
100	16.4	1.64	3	5.0	---
100	16.4	1.64	3	5.0	1.5

Surface visualization revealed large vertical undulations of the weld pool surface. Cross-sections of several samples indicated that the surface depression noted earlier was considerably deeper and more conical in shape than at lower power levels. Figure 19 is a photograph of a typical solidified weld pool at this power level. Weld pool development curves shown in Figures 20 and 21 indicate that weld reached a steady state size of 13.0 millimeters between

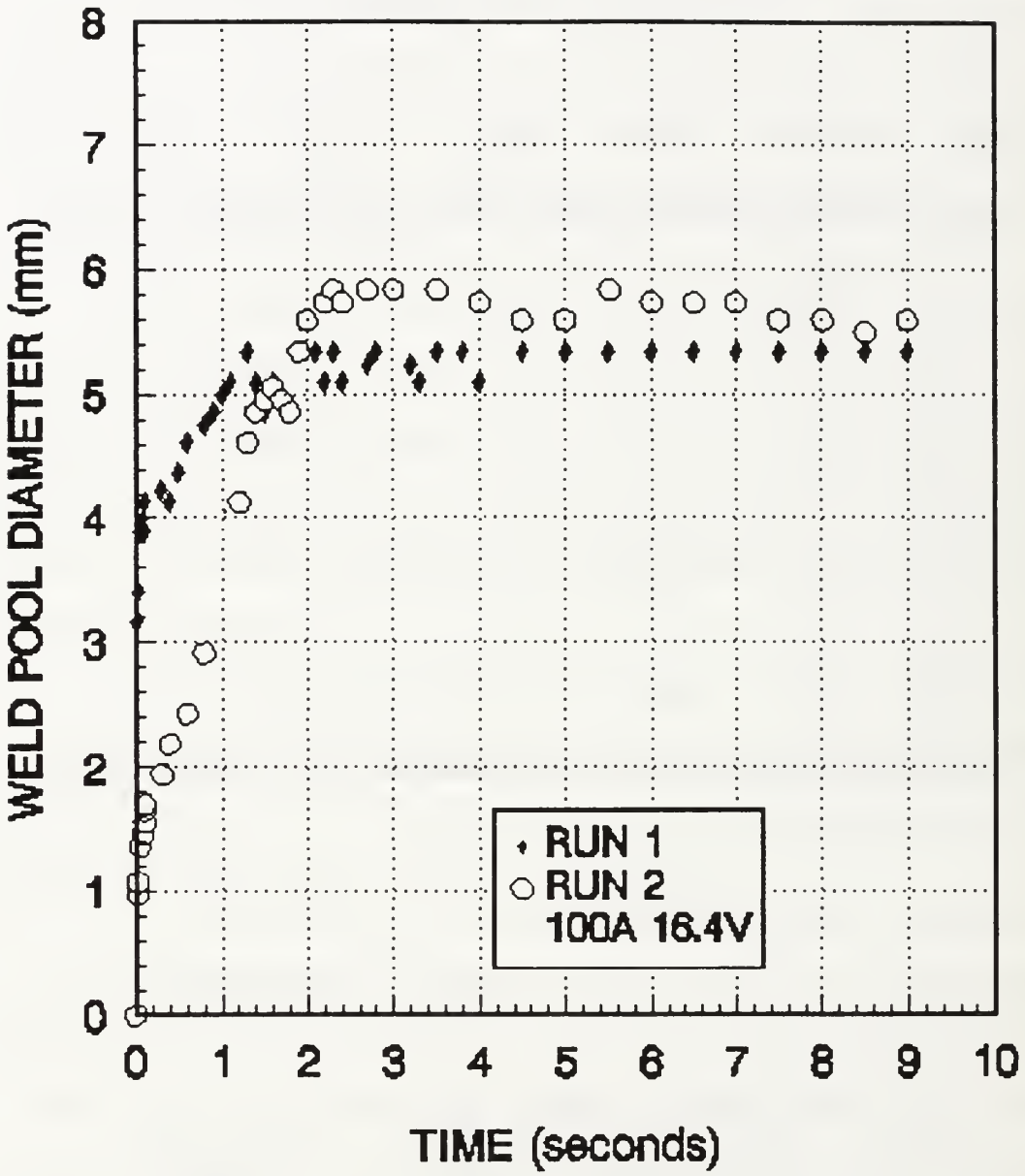

FIGURE 14. Weld Pool Growth Rate With Time For 6061 Aluminum Low Current Welds. 45 Degree Electrode Tip Angle, 3 mm Arc Length.

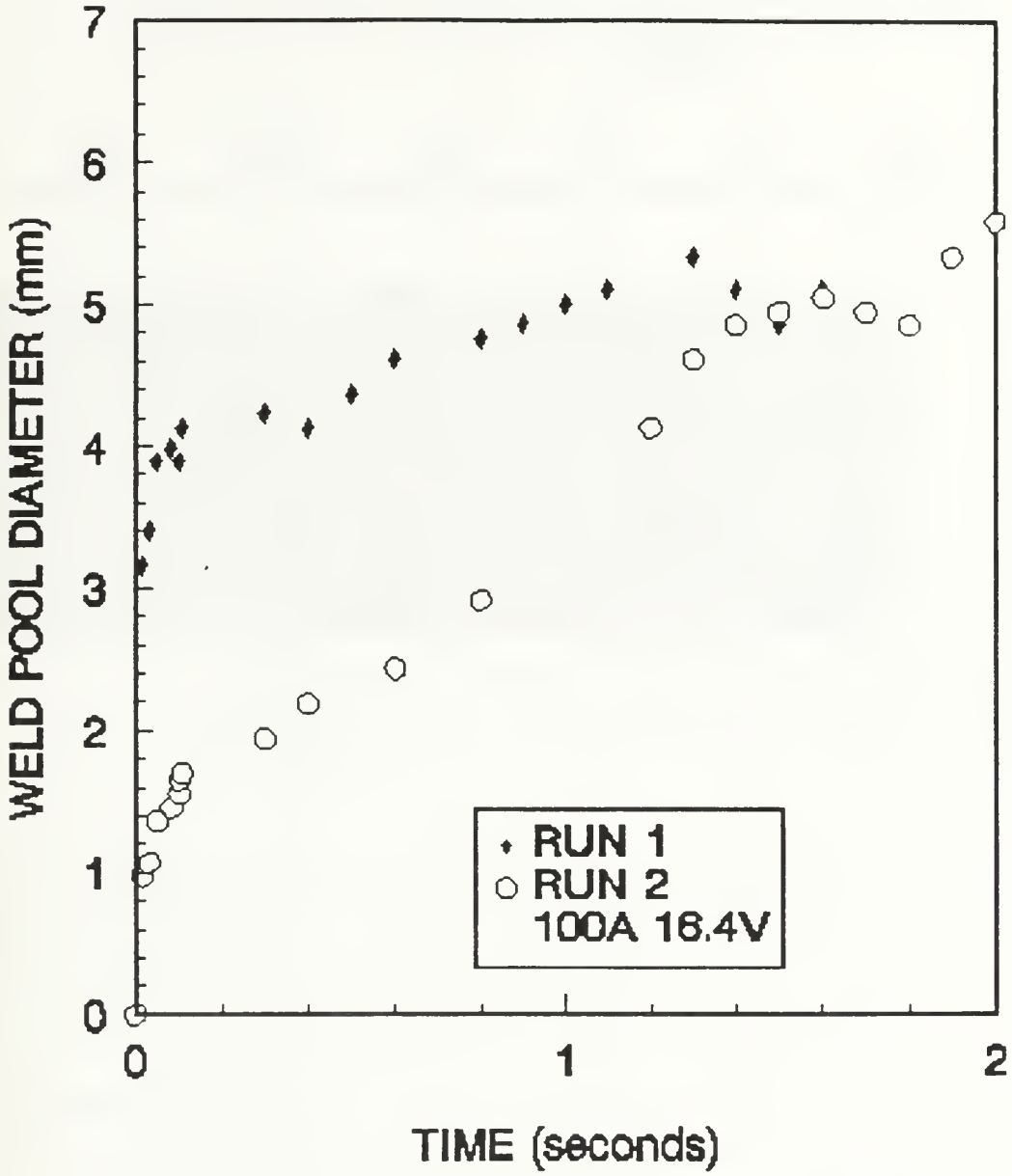

FIGURE 15. Weld Pool Growth Rate With Time For 6061. Expansion of 0-2 Second Interval From Figure 14. Aluminum Low Current Welds. 45 Degree Electrode Tip Angle, 3 mm Arc Length.

TABLE VII . SUMMARY LISTING OF MEDIUM CURRENT STATIONARY ARC EXPERIMENTS ON 6061 ALUMINUM.

I (Amps)	V (Volts)	Power (Kwatts)	Arc Length (mm)	Weld Pool Diameter (mm)	Pool Depth (mm)
150	11.2	1.68	3	4.8	1.5
150	11.2	1.68	3	5.0	7.0
150	11.2	1.68	3	4.9	2.5
150	11.2	1.68	3	5.1	1.5
150	11.2	1.68	3	5.5	1.8
150	11.2	1.68	3	6.0	2.0
150	11.2	1.68	3	5.8	2.25
150	11.2	1.68	3	7.0	---
150	11.2	1.68	3	6.4	---
150	11.2	1.68	3	6.0	---
150	11.2	1.68	3	6.0	---
150	11.2	1.68	3	6.0	---
150	11.2	1.68	3	5.8	---
150	11.3	1.695	3	7.0	---
150	11.3	1.695	3	6.8	---
150	11.3	1.695	3	6.5	---
150	11.3	1.695	3	6.4	---
150	11.3	1.695	3	5.8	---
150	11.3	1.695	3	6.2	---
150	11.3	1.695	3	6.2	---
150	11.3	1.695	3	6.5	---
150	11.3	1.695	3	6.2	---
150	11.3	1.695	3	6.0	---
150	11.3	1.695	3	6.5	---

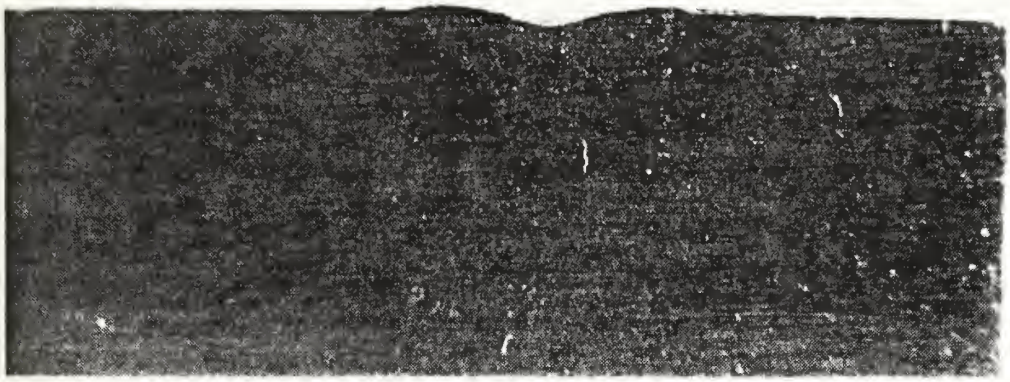

Figure 16. Etched Section Showing Inflection Of 6061 Fusion Zone Interface. 150A, 11.2V, 5.53 mm Pool Diameter, 1.8mm Penetration Depth. Enlargement x7.55.

6.5 to 7 seconds. The timewise growth curves for the three power levels are collected in Figure 22.

C. WELDING EFFICIENCY

Welding efficiency was calculated for selected welds using Rosenthal's [Ref. 15 and 16] point source solution evaluated for stationary welds as follows:

$$\eta = \frac{2\pi (T_m - T_0) k r_0}{EI} \qquad (2)$$

where
- k = average thermal conductivity (W/m-K)
- T_m = melting temperature of the material (K)
- T_0 = ambient temperature (K)
- I = current (A)
- E = voltage (V)
- r_0 = distance from the point source $(x^2+y^2+z^2)^{1/2}$ (m)

The values of k, T_m, and T_0, were considered to be constant for the purpose of this calculation. For HY-80 T_m was equal to 1810K [Ref. 17], T_0 was 298K and k was 30 W/m-K [Ref. 18]. For 6061 aluminum T_m was 850K and k was equal to 180 W/m-K [Ref. 12].

Table IX contains a comprehensive listing of efficiencies calculated using the above equation. It should be noted that efficiency is highly dependent on the value chosen for r_0. This explains the large deviation between efficiencies calculated using the weld penetration depth (r_p) and those determined with the weld pool radius (r_d).

TABLE VIII . SUMMARY LISTING OF HIGH CURRENT STATIONARY ARC EXPERIMENTS ON 6061 ALUMINUM.

I (Amps)	V (Volts)	Power (Kwatts)	Arc Length (mm)	Weld Pool Diameter (mm)	Pool Depth (mm)
170	11.5	1.995	3	12	---
170	11.5	1.995	3	16	---
170	11.5	1.995	3	12	---
170	11.5	1.995	3	12	---
170	11.5	1.995	3	12.5	---
170	11.5	1.995	3	13	---
170	11.5	1.995	3	12	---
170	11.5	1.995	3	13	8.0
170	11.5	1.995	3	11	---
170	11.5	1.995	3	12	---
170	11.5	1.995	3	11.5	8.0
170	11.5	1.995	3	12	---
170	11.5	1.995	3	18	8.5
170	11.5	1.995	3	12	---
170	11.5	1.995	3	19	---
170	11.5	1.995	3	13	---
170	11.5	1.995	3	12	---
170	11.5	1.995	3	12.5	6.5
170	11.5	1.995	3	12	---
170	11.5	1.995	3	12.5	---
170	11.5	1.995	3	13	6.5
170	11.5	1.995	3	12.5	---
170	11.5	1.995	3	14	8.5
170	11.5	1.995	3	12.5	---

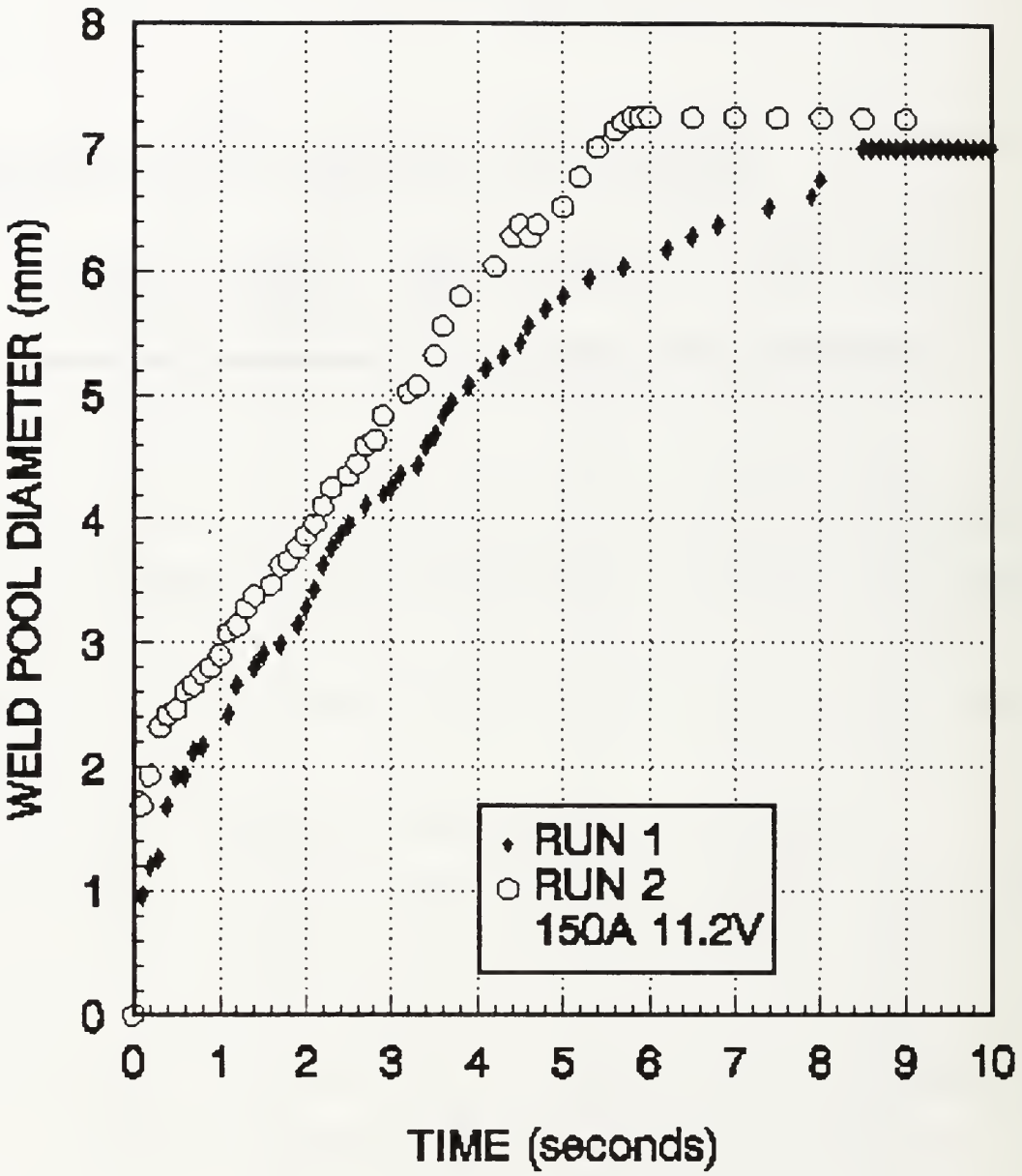

FIGURE 17. Weld Pool Growth Rate With Time For 6061 Aluminum Medium Current. 45 Degree Electrode Tip Angle, 3 mm Arc Length.

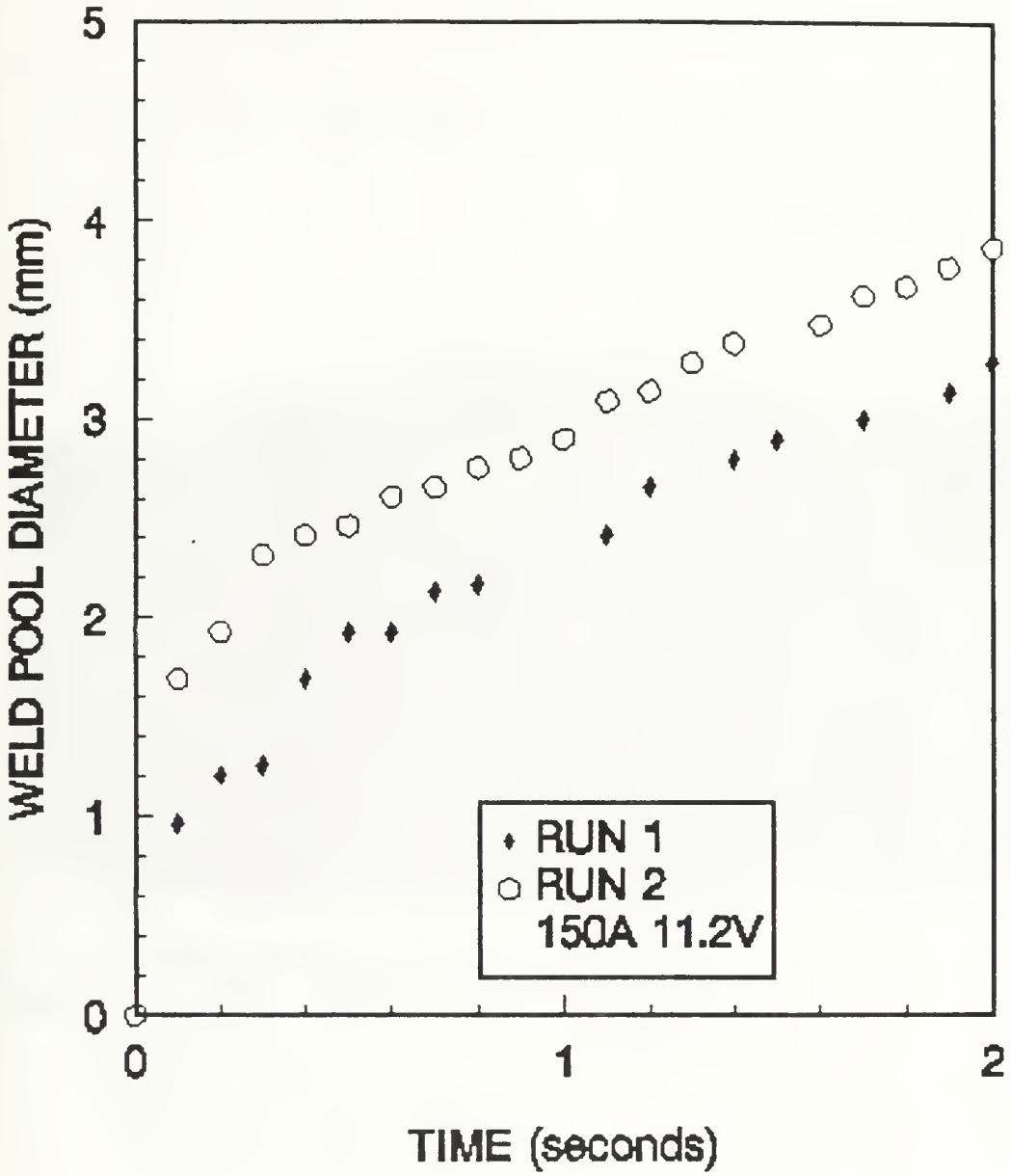

FIGURE 18. Weld Pool Growth Rate With Time For 6061. Expansion of 0-2 Second Interval From Figure 17 Aluminum Medium Current. 45 Degree Electrode Tip Angle, 3 mm Arc Length.

FIGURE 19. Weld Pool Crossection Showing Large Conical Depression At High Current. 170A, 11.5V, Pool Diameter 12 mm, Penetration 6.5 mm. Enlargement x7.8 Times.

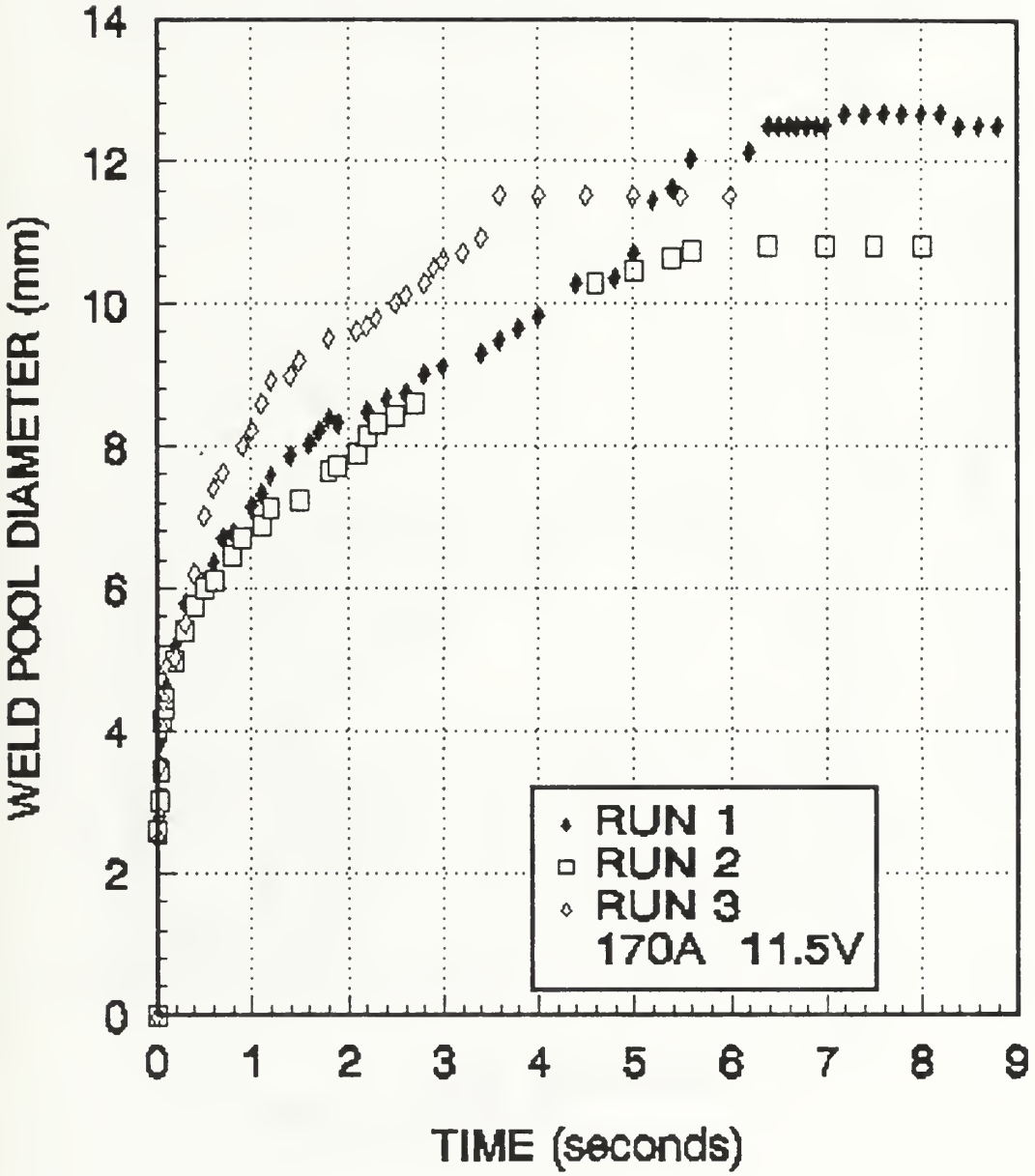

FIGURE 20. Weld Pool Growth Rate With Time For 6061 Aluminum High Current. 45 Degree Electrode Tip Angle, 3 mm Arc Length.

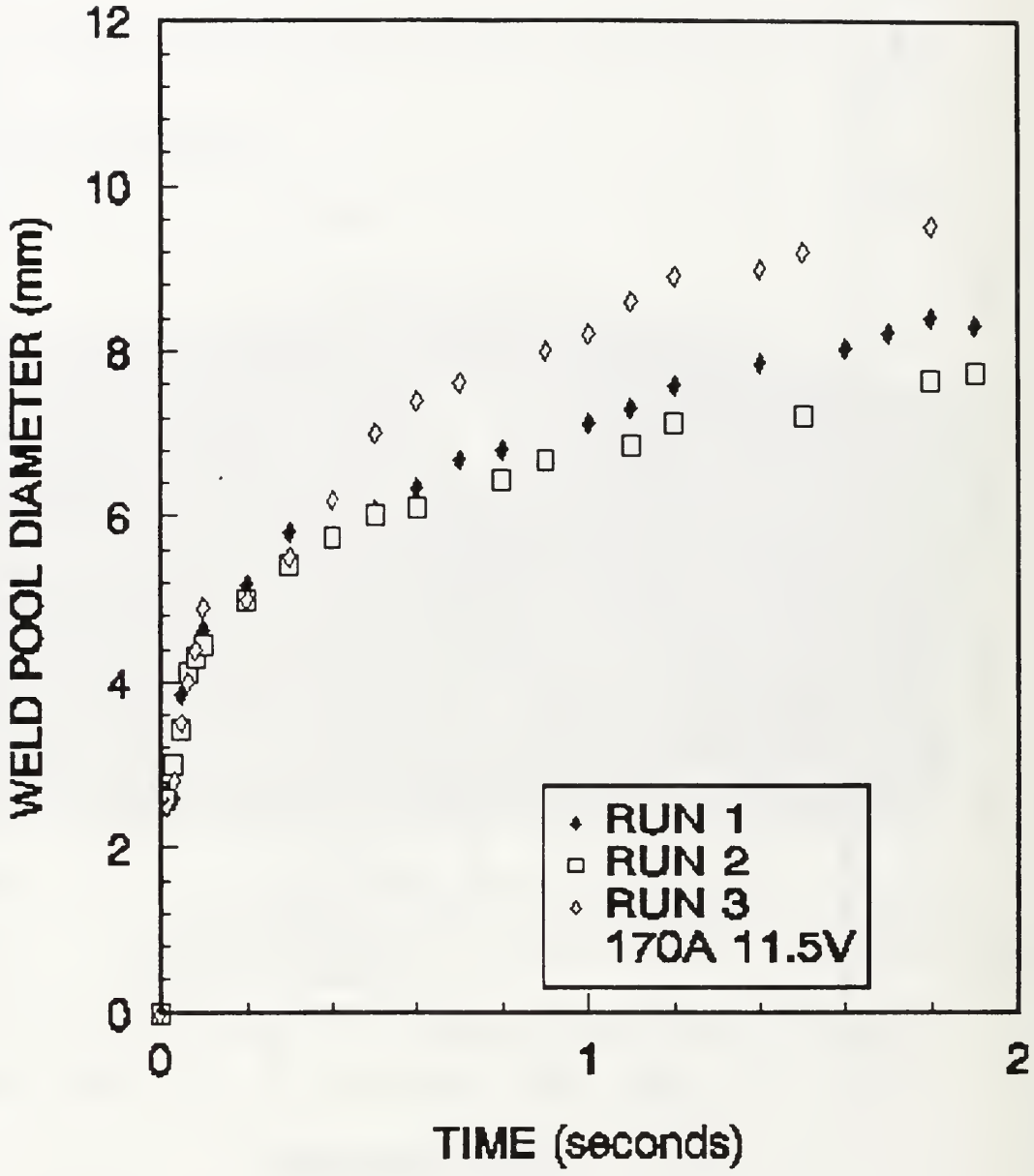

FIGURE 21. Weld Pool Growth Rate With Time For 6061. Expansion of 0-2 Second Interval From Figure 20. Aluminum High Current. 45 Degree Electrode Tip Angle, 3 mm Arc Length.

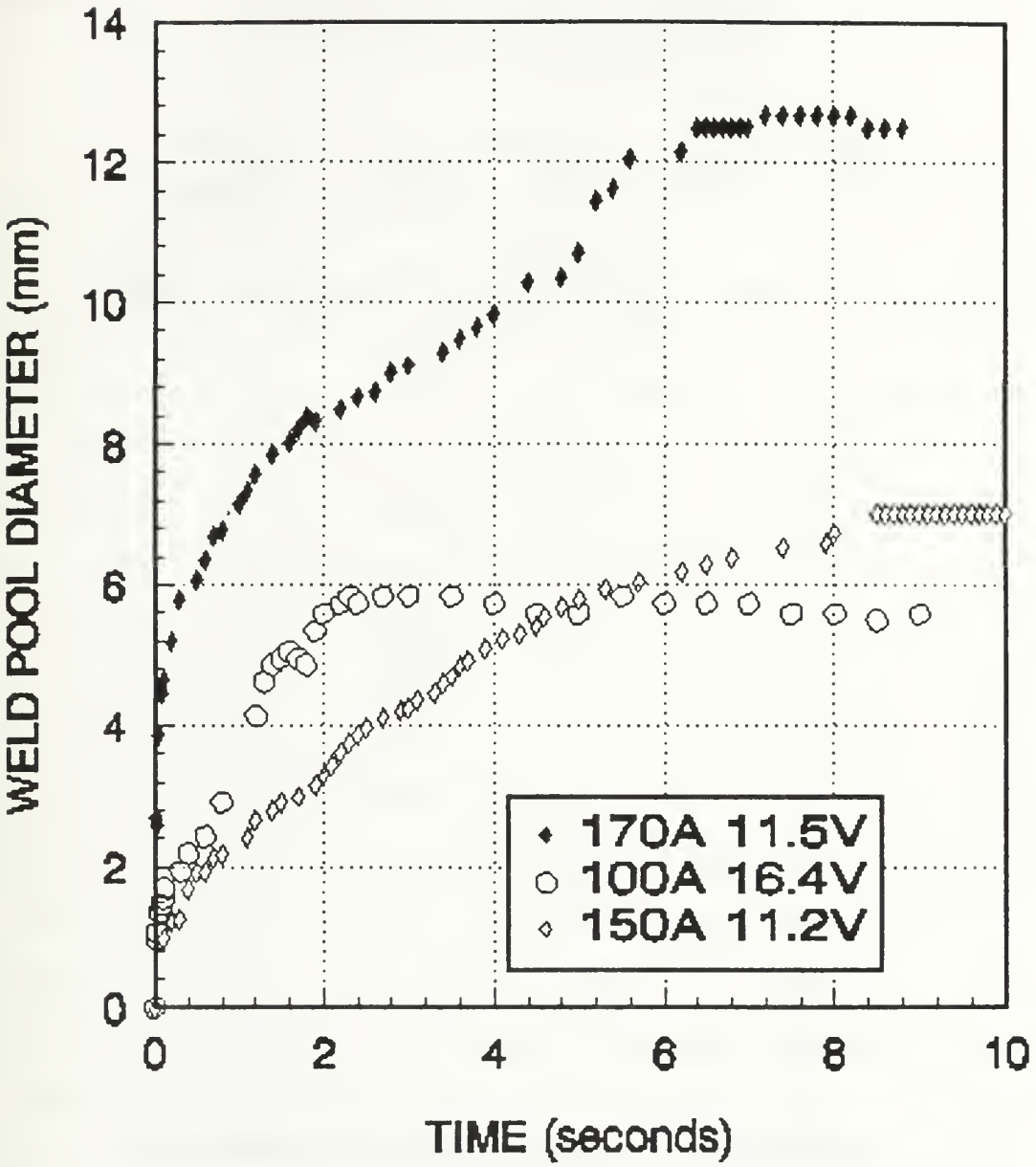

FIGURE 22. Weld Pool Growth Rate With Time For 6061 Aluminum Low, Medium, and High Current. 45 Degree Electrode Tip Angle, 3 mm Arc Length.

TABLE IX. SUMMARY LISTING OF CALCULATED EFFICIENCIES FOR STATIONARY ARC EXPERIMENTS ON 6061 ALUMINUM.

POWER (Kwatts)	WELD POOL DIAMETER (mm)	PENETRATION DEPTH (mm)	EFFICIENCY BASED ON DIAMETER (percent)	EFFICIENCY BASED ON PENETRATION (percent)
1.115	3.0	1.0	83.9	55.9
1.115	4.5	1.0	*	55.9
1.115	3.5	1.5	97.9	83.9
1.115	2.4	0.5	67.18	27.9
1.115	3.9	1.0	*	55.9
1.640	5.0	1.5	*	83.9
1.680	4.8	1.5	89.0	55.7
1.680	5.0	2.0	92.9	74.3
1.680	4.9	2.5	91.0	92.9
1.680	5.10	1.5	94.7	55.7
1.680	5.5	1.8	*	66.9
1.680	6.0	2.0	*	74.3
1.680	5.8	2.25	*	83.6
1.995	13.0	8.0	*	*
1.995	11.5	8.0	*	*
1.995	18.0	8.5	*	*
1.995	12.5	6.5	*	*
1.995	13.0	6.5	*	*
1.995	14.0	8.5	*	*

* Values above 100% indicate Rosenthal's Point source solution is poor representation of the fusion zone size.

IV. MOVING ARC EXPERIMENTS

Moving welds on 30.5 cm diameter by 2.54 cm thick circular HY-80 steel plates and 28 cm by 17.75 cm by 1.25 cm thick rectangular 6061 aluminum plates are considered in this chapter. Welds were conducted at low, medium, and high input current ranges and several speeds for both materials. Welds on HY-80 were conducted to determine the effect of the asymmetric current path on surface flow patterns. Experiments on 6061 aluminum were performed in order to study flow characteristics and the effect of arc movement on efficiency.

A. HY-80 STEEL

Moving arc runs began at a location 5.0 cm from the center of the circular plate and progressed away from the center along a radial line as described in Chapter II. Speeds of 1.79, 0.967, and 0.627 mm/s were used. Shielding Gas (argon) flow rate was maintained at a constant .0708 cubic meters per hour for all experiments. Weld pool dimensions were measured directly from the video monitor screen then converted to an actual dimension using either the gas cone or the tungsten electrode as a scale (gas cone was 17mm diameter, electrode was 3mm diameter). Uncertainty in the dimensions was 0.2mm. Table X contains a summary

TABLE X . SUMMARY LISTING OF MOVING ARC EXPERIMENTS ON HY-80 STEEL.

I (Amps)	V (Volts)	Power (Kwatts)	Arc Length (mm)	Weld Pool Length (mm)	Pool Width (mm)	Arc Speed (mm/sec)
110	11.2	1.232	3	5.5	4.5	1.79
110	11.2	1.232	3	6.0	5.0	.967
110	11.2	1.232	3	5.0	4.5	.627
170	11.2	1.904	3	8.5	8.0	.760
170	11.2	1.904	3	6.5	5.0	.967
170	11.2	1.904	3	8.0	7.5	.627
200	11.7	2.34	3	10.0	9.0	.626
200	11.7	2.34	3	8.0	6.0	.967
200	11.7	2.34	3	10.0	9.0	.760
240	12.3	2.952	3	11.0	16.0	.627
240	12.3	2.952	3	11.5	15.0	.760
240	12.3	2.952	3	12.0	8.5	2.85

listing of welding parameters and results for all moving welds on HY-80.

1. LOW CURRENT EXPERIMENTS

Low current welds were conducted at 110 Amps, 11.2 Volts. Flow patterns at this power level were laminar in nature with no rotation within the weld pool observed. Welding speed and position relative to the ground connection located at the center of the pool had no apparent effect. Weld pool shape was elliptical in nature with a build up of material at the initiation site and a pool depression forming at the point of arc cessation. Material was removed from the front of the pool, circulated along the side and

then was deposited at the rear of the pool. Both characteristics were described by Espinosa [Ref. 8].

2. MEDIUM CURRENT EXPERIMENTS

Welds were conducted at 170 Amps, 11.2 Volts, and 200 Amps, 11.7 Volts. Flow patterns exhibited more vigorous flows than at the low power levels. Rotation occurred on a sporadic basis near the outside of the plate for several cases. Variation in welding speed and power level appeared to have minimal effect on flow patterns. Circulation was from the front to the rear along both sides of the pool.

3. HIGH CURRENT EXPERIMENTS

240 Amps, 12.3 Volts was used for all welds in this range. Highly vigorous flow patterns appearing to be turbulent existed with sporadic rotation at random locations along the weld bead. Circulation of pool material was from front to rear along both sides of the pool. Pool shape was elliptical with a build up of material at the weld initiation point and a pool depression at the point of cessation as also observed for lower currents. Variation of arc speed affected only the width of the weld pool. Flows at the different arc speeds were similar in nature to each other.

B. 6061 ALUMINUM

Moving bead on plate arc experiments were conducted as described in Chapter II. Plate dimensions were identical to

those used in stationary welds. Three power levels of 1.39, 2.07, and 2.26kW were considered with arc speeds of 0.626, 0.967, and 1.795 mm/s at each power level. Argon shielding was used at a constant of rate 0.1416 cubic meters per hour. Table XI contains a summary of parameters and results for all aluminum experiments.

TABLE XI . SUMMARY LISTING OF MOVING ARC EXPERIMENTS ON 6061 ALUMINUM.

I (Amps)	V (Volts)	Power (Kwatts)	Arc Length (mm)	Weld Pool Width (mm)	Pool Length (mm)	Arc Speed (mm/sec)	Pool Depth (mm)
105	13.2	1.39	3	4.0	5.5	.627	1.5
105	13.2	1.39	3	4.0	5.5	.627	2.0
105	13.2	1.39	3	5.0	6.5	.627	1.6
105	13.2	1.39	3	4.0	7.0	.967	1.5
105	13.2	1.39	3	4.0	6.5	.967	1.8
105	13.2	1.39	3	4.0	7.0	1.79	1.9
150	13.8	2.07	3	5.5	7.5	.627	2.8
150	13.8	2.07	3	6.0	9.0	.967	1.8
150	13.8	2.07	3	6.5	8.5	.967	---
150	13.8	2.07	3	5.0	10.0	1.79	1.5
150	13.8	2.07	3	9.0	5.5	1.79	2.0
170	13.3	2.26	3	8.5	---	.627	---
170	13.3	2.26	3	12.0	12.5	.627	4.0
170	13.3	2.26	3	13.0	---	.967	---
170	13.3	2.26	3	13.0	12.0	.967	3.8
170	13.3	2.26	3	13.0	---	.179	---
170	13.3	2.26	3	11.0	10.0	.179	3.0

Immediately upon the commencement of arc motion the weld pool shape changed from circular to an elliptical shape with a depressed surface directly below the electrode. Oxide particles were observed migrating from the front of the weld area down into the pool depression and then directly to the rear. Surface flows displayed no circumferential motion and material did not solidify in a uniform fashion as with steel welds. Instead, an extremely uneven surface formed with many irregularities as illustrated in Figure 23. The center weld bead also shows the weld pool depression that forms at the point of cessation of the arc (located at the right of the photograph). Pool depression was very prominent in a majority of moving arc welds on aluminum and was, in general much more severe than in the steel tests. These features were common to all welding powers and arc speeds.

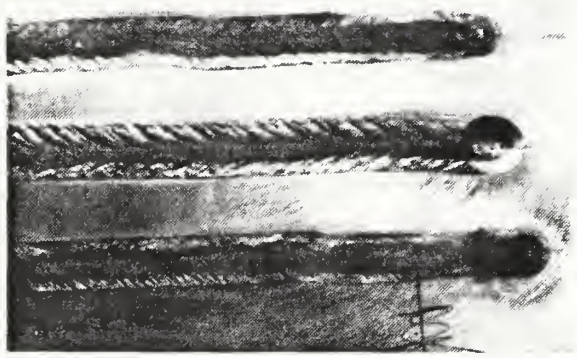

FIGURE 23. Solidified Weld Bead on 6061 Aluminum Illustrating Weld Pool Rise, Depression, and Uneven Surface. 170A, 13.3V.

Figure 24 is a photograph of a typical fusion zone shape that resulted from moving welds on aluminum. Note that the sector of a circle shape is in agreement with many of the numerical models mentioned earlier.

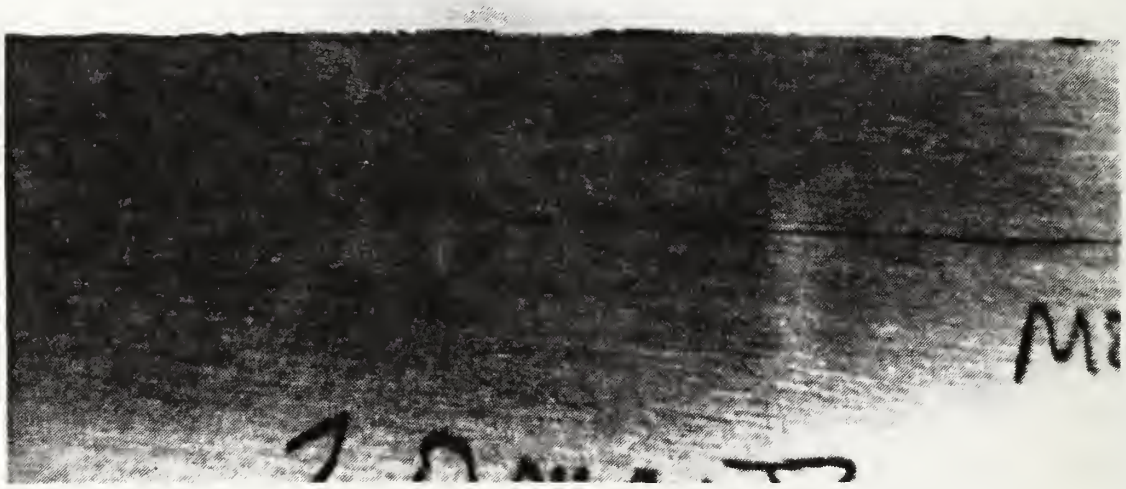

Figure 24. Fusion Zone Of Moving Arc Weld On 6061 Aluminum. 150A, 11.2V, 2.0mm Penetration, 5.2 mm width, Welding Speed 1.78 mm/sec. Enlargement 6.3 times.

C. WELDING EFFICIENCY

Welding efficiency for moving welds in 6061 can be determined using Rosenthal's [Ref. 15] point source heat flow equation as follows:

$$\eta = \frac{2\pi (T_m - T_0) k r_0}{IE} \exp \frac{V(r_0 + X)}{2\alpha} \qquad (3)$$

where k = average thermal conductivity (W/m-K)

T_m= melting temperature of the material (K)

T_0= ambient temperature (K)

I = current (A)

E = voltage (V)

r_0= distance from the point source $(x^2+y^2+z^2)^{1/2}$ (m)

V = welding speed (m/s)

α = thermal diffusivity (m^2/s)

X = distance parallel to welding direction, from the point source. (m)

Equation 3 and measurements of actual weld pool dimensions obtained from videos and solidified weld pools enabled calculation of this parameter directly. Table XII is a listing of efficiencies computed for specific cases. Most of the values of efficiency range between 81% to 94% which compare favorably to a study by Giedt et al. [Ref. 16]. It should be noted that the efficiency values in that study were obtained by calorimetric measurements and not by the use of the point source solution.

TABLE XII. SUMMARY LISTING OF CALCULATED EFFICIENCIES FOR MOVING ARC EXPERIMENTS ON 6061 ALUMINUM.

POWER (Kwatts)	SPEED (mm/sec)	% FRONT	% REAR	% SIDE	% BOTTOM
1.39	.623	44.9	*	90.9	68.1
1.39	.623	91.4	*	91.4	91.4
1.39	.623	*	*	*	73.2
1.39	.967	*	*	92.8	69.4
1.39	.967	8	*	92.7	83.3
1.39	1.79	*	*	90.3	85.7
2.07	.623	*	*	77.4	*
2.07	.97	*	*	*	*
2.07	.97	*	*	*	*
2.07	1.79	*	*	*	81.6
2.07	1.79	*	*	*	92.0
2.26	.63	93.0	59.3	*	---
2.26	.63	93.7	*	*	*
2.26	.97	*	*	*	---
2.26	.97	*	*	*	*
2.26	1.79	*	*	*	*
2.26	1.79	89.0	*	*	89.1

* Values above 100% indicate Rosenthal's Point source solution is poor representation of the fusion zone size.

V. CONCLUSIONS

Accurate numerical models of the Gas Tungsten Arc Welding process are essential for automatic adaptive control to be successful. Current models do not account for a variety of parameters and may require modification to account for experimental observations. Experiments in this study utilized a laser vision system to study weld pool free surface flow patterns during welding of HY-80 steel and 6061 aluminum.

Observations of HY-80 stationary welding experiments indicate several key features that should be accounted for. First, current path geometry plays a significant role in the surface flows induced in a weld pool. A symmetric current path effectively eliminated stirring within the pool. Secondly, stationary welds conducted at low current levels exhibited a periodic pulsing motion that is clearly a transient feature not predicted by present studies which model the weld pools assuming a steady state condition. Finally, inflection points in the observed weld pool fusion interface indicate partial agreement with Zacharia [Ref.13].

Moving arc experiments on HY-80 steel indicated that a symmetric current path geometry nearly eliminated rotation within the weld pool. The weld pool assumed an elliptical

shape during moving welds and exhibited a pool depression. Both features were observed by Espinosa [Ref. 8.].

Studies on stationary 6061 aluminum welds show some interesting and quite unique features that contrast experiments on HY-80. A surface oxide layer forms on aluminum welds and appears to play a major role in the shape and type of flows that result. Weld pool models assume that a free surface exists and do not account for this fact. Large weld pool depressions form in the solidified fusion zone in contrast to a significant pool rise in steel welds. In addition a slow vertical undulation of the pool that was not seen in other materials was noted. Transient in nature it is not predicted by numerical studies. Also, slow rotational flows beneath the oxide layer were present. The Lorentz force is a possible driving mechanism for this motion as all welds on 6061 contained asymmetric current path geometry. These features most certainly have a profound effect on motion and heat transfer within the pool.

Moving arc experiments on 6061 aluminum indicated an elliptical pool shape similar to that seen in HY-80 welds. Weld pool depression was also present in the aluminum tests but it was more severe than steel welds. As with stationary 6061 experiments a surface oxide layer formed and should be accounted for in numerical models.

LIST OF REFERENCES

1. Oreper, G.M., and Szekely, J., "Heat and Fluid-Flow Phenomena in Weld Pools," Journal of Fluid Mechanics, Vol. 147, pp. 53-79, 1984.

2. Saedi, H.R., and Unkel, W., "Thermal-Fluid Model for Weld Pool Geometry Dynamics," Journal of Dynamic Systems, Measurement, and Control, Vol. 111, pp. 268-276, June 1989.

3. Zacharia, T., Eraslan, A.H., Aidun, D.K., and David, S.A., "Three-Dimensional Transient Model for Arc Welding Process," Metallurgical Transactions B, Vol. 20B, pp. 645-659, October 1989.

4. Kim, S.D., and Na, S.J., "A Study on Heat and Mass Flow in Stationary Gas Tungsten Arc Welding Using the Numerical Mapping Method," Journal of Engineering Manufacture, Part B., pp. 233-242, 1989.

5. Woods, R.A., and Milner, D.R., "Motion in the Weld Pool in Arc Welding", Welding Journal, pp. 163-173, April 1971.

6 Malinowski-Brodnicka, M., Ouden, G. den., and Vink, J.P., "Effect of Electromagnetic Stirring on GTA Welds in Austenite Stainless Steel," Welding Journal, pp. 525-595, February 1990.

7. Espinosa, Daniel C., "Visualization of Gas Tungsten Arc Weld Pools," Master's Thesis, Naval Postgraduate School, Monterey, California, 1991.

8. "Welding Handbook", American Welding Society, Vol. 1, Eighth Edition, pp. 47-50, 1991.

9. "System Description and Operating Instructions," Laser-Augmented Welding Vision System, Control Vision, Inc., Idaho Falls, Idaho.

10. Model UV12 Nitrogen Laser Service Manual, PRA Laser Inc., November 1987.

11. Model A6-6720-P Time Lapse SVHS Recorder, Panasonic Communications and Systems Company.

12. "Structural Alloys Handbook," Department of Defense, Vol. 3, 1989 Edition.

13. Zacharia, T., David, S.A., Vitek, J.M., and Debroy, T., "Weld Pool Development During GTA and Laser Beam Welding of Type 304 Stainless Steel, Part 1, Theoretical Analysis," Welding Journal, pp. 4995-5095, December 1989.

14. Wang, Y.H., and Kou, S., "Driving Forces for Convection in Weld Pools," Advances in Welding Sciences and Technology, p. 65, May 1986.

15. Rosenthal, D., "The Theory of Moving Sources of Heat and Its Application to Metal Treatments," Transactions of the ASME, November 1946.

16. Giedt, W.H., "GTA Weld Penetration and Effects of Deviations in Machine Variables," Sandia National Laboratories Report, June 1987.

17. Incropera, F.P. and DeWitt, D.P., "Introduction to Heat Transfer," John Wiley & Sons, Inc., 1985.

18. Ule, R.L., "A Study of the Thermal Profiles During Autogenous Arc Welding," M.S. and M.E. Thesis, Naval Postgraduate School, Monterey, California, March 1989.

INITIAL DISTRIBUTION LIST

		No. of Copies
1.	Defense Technical Information Center Cameron Station Alexandria, VA 22304-6145	2
2.	Library, Code 52 Naval Postgraduate School Monterey, CA 93943-5002	2
3.	E.A. Metzbower Naval Research Laboratory Washington, D.C. 20375-5000	1
4.	Department Chairman, Code 69 Department of Mechanical Engineering Naval Postgraduate School Monterey, CA 93943-5000	1
5.	Yogendra Joshi, Code ME/Ji Naval Postgraduate School Monterey, CA 93943-5000	2
6.	Richard Morris Code 2815 David Taylor Research Laboratory Annapolis, MD 21402	1
7.	RADM Millard Firebaugh SEA-05 Naval Sea Systems Command Washington, D.C. 20362-5101	1
8.	SEA-92R Naval Sea Systems Command Washington, D.C. 20362-5101	1
9.	Naval Engineering Curricular Office Code 34 Naval Postgraduate School Monterey, CA 93943-5000	1

10. LT Peter Schupp 3
Pearl Harbor Naval Shipyard
Pearl Harbor, HI 96860-5350

Thesis
S36852 Schupp
c.1 Weldpool flow visual-
ization studies during
gas tungsten arc welding
of steel and aluminum.

Thesis
S36852 Schupp
c.1 Weldpool flow visual-
ization studies during
gas tungsten arc welding
of steel and aluminum.

AMERICAN BINDERY 1 10-93

DUDLEY KNOX LIBRARY
3 2768 00018478 2